A

MAJOR PROJECT REPORT

ON

EMG CANCELLATION FROM ECG SIGNAL USING MODIFIED NLMS ADAPTIVE FILTERS

BY

V.SRIKAR(16SS1A0456)

Under the guidance of

Sri V.RAJANESH

Department of Electronics and Communication Engineering

Jawaharlal Nehru Technological University Hyderabad

College of Engineering Sultanpur

pulkal (M), Sangareddy-502293, Telangana

2020

EMG CANCELLATION FROM ECG SIGNAL USING MODIFIED NLMS ADAPTIVE FILTERS

A

MAJOR-PROJECT REPORT
SUBMITTED IN PARTIAL FULFILLMENT
OF THE REQUIREMENTS FOR THE DEGREE OF
BACHELOR OF TECHNOLOGY
IN
ELECTRONICS AND COMMUNICATION ENGINEERING
BY

V.SRIKAR (16SS1A0456)

UNDER THE GUIDANCE OF

Sri V.RAJANESH

Department of Electronics and Communication Engineering
Jawaharlal Nehru Technological University Hyderabad
College of Engineering Sultanpur
pulkal (M), Sangareddy-502293, Telangana

2020

Jawaharlal Nehru Technological University Hyderabad

College of Engineering Sultanpur

pulkal (M), Sangareddy-502001, Telangana

Department of Electronics and Communication Engineering

CERTIFICATE

Date:

This is to certify that the project work entitled ***EMG CANCELLATION FROM ECG SIGNAL USING MODIFIED NLMS ADAPTIVE FILTERS*** *is a bonafide work carried out by* ***V.SRIKAR***
bearing Roll No ***(16SS1A0456)****in partial fulfillment of the requirements for the degree of* ***BACHELOR OF TECHNOLOGY*** *in* ***ELECTRONICS & COMMUNICATION ENGINEERING*** *by the Jawaharlal Nehru Technological University, Hyderabad during the academic year 2020.*

Sri V.RAJANESH
Project Guide

Dr. Y. Raghavender Rao
Head of the department

Mr. Devisingh
Project Co-Guide

ACKNOWLEDGMENT

We wish to take this opportunity to express our deep gratitude to all those who helped, encouraged, motivated and have extended their cooperation in various ways during our major-project work. It is our pleasure to acknowledge the help of all those individuals who were responsible for foreseeing the successful completion of our project.

We express sincere gratitude to **Dr. B. BALU NAIK** Principal of JNTUHCES for his support during the course period.

We sincerely thank **Dr. V. VENKATESWARA REDDY,** the Vice Principal of JNTUHCES for his kind help and cooperation.

We are thankful to **Dr. Y. RAGHAVENDER RAO**, Professor and Head of the Department of Electronics and Communication Engineering of JNTUHCES for his effective suggestions during the course period.

We would like to express our gratitude to **Sri V. RAJANESH**, Assistant Professor, for his guidance and constant supervision.

Finally, we would like to express our gratitude to **Mr. DEVISINGH** , for spendinghis valuable time and providing their guidance throughout the course period.

BY

V.SRIKAR(16SS1A0456)

TABLE OF CONTENTS

LIST OF FIGURE

LIST OF TABLE

ABSTRACT

In this study, improved normalized LMS adaptive filters are proposed to reduce the electromyogram (EMG) noise from ECG signals. The proposed technique mainly uses simple addition and shift operations and achieves considerable speed over other methods based on the LMS method. Simulation result gives by the improved versions ofadaptive filter (NLMS) show superior performance to be compared with other technique such as wavelet and empirical mode decomposition.

Keywords—ECG signal; adaptive filter; proportionate; improved proportionate;NLMS

CHAPTER 1
INTRODUCTION

1.1 Intoduction

The most common sources of noise contamination in ECG signals are Baseline Wander (BW), Powerline Interference (PLI), Electromyogram (EMG) and motion artifact (MA). Baseline wander noise comes from multiple numbers of skin electrodes and human respiration systems . The 50 or 60 Hz interference from mains power supply, also referred to as powerline interference, prevents a clean reading from ECG signals . EMG measures the electrical activity of muscles at rest and during contraction and retaining an ECG signal along with EMG noise may result an incorrect prediction of cardiac activities. Motion artifact is interference resulting from muscle movement at the electrodes which are placed onto the patient's skin and could produce large amplitude signals in the ECG which can then be misinterpreted and misdiagnosed . Therefore, noise reduction becomes the first phase in order to process the signals of an electrocardiograph (ECG).

The BW, PLI and EMG noises are uncorrelated to the ECG signal unlike the MA whose noise spectrum is correlated to the ECG signal , thus making it the most difficult type of noise to remove. Several adaptive filtering techniques for implementing noise cancellation have been reported. Deng et al showed that adaptive filters are capable of identifying sparse impulse response . In this study, the Proportionate Normalized Least Mean Square PNLMS is used to set a different step size for different coefficients based on the optimum magnitudes. Adaptive filters are also widely used in acoustic echo cancellation (AEC) . Normally, the step-size parameter of adaptive filters varies depending on situations where a double talk and an echo path change occur. Other’s proposed a controllable step-size parameter for the situation when double talk and echo path changes occur simultaneously. Here, the optimal step-size parameter is employed from the output of the sub-adaptive filter and the echo path change detector which is controlled via the double talk detector.

Adaptive filters were also used in stock market prediction . Hybrid adaptive filters were able to estimate predicted values of the five largest stock markets, namely, BSE100, NASDAQ, NIKKEI225, S&P NIFTY, and FTSE100. In medical applications, Thakor& Zhu used least mean square adaptive filter algorithms to reduce the BW, PLI and EMG noises in ECG signal. Adaptive filters have also been used to filter the ocular and facial muscles artifact in order to produce a clean electroencephalogram (EEG) signal . The work of Rahman et al in adaptive filters for reducing noise in ECG signals applied a Normalized Signed Regress or LMS (NSRLMS) algorithm to obtain clean signals . Rahman et al stated that signed input signals during weight updating period may increase the performance of the filter. However, they found a better technique to deal with corrupted ECG signals by using a Constrained Stability Least Mean Squares (CSLMS) algorithm but they only filter the BW and PLI noises . This resulted in a better overall output than NSRLMS, but some distortion was still present and needed to be removed. In this paper, we concentrate in the reduction of electromyogram noise in ECG signals. A number of adaptive LMS-based filters, such as Normalized Least Mean Square (NLMS), Proportionate NLMS (PNLMS), Improved PNLMS (IPNLMS) and μ-PNLMS (MPNLMS), are used in order to reduce the electromyogram noise from the ambulatory ECG signal. The signals used, were recorded using a 3-lead Holter monitor and were: augmented vector foot (aVf), augmented vector left (aVl) and augmented vector right (aVr), attached to a human body as shown in Figure 1.

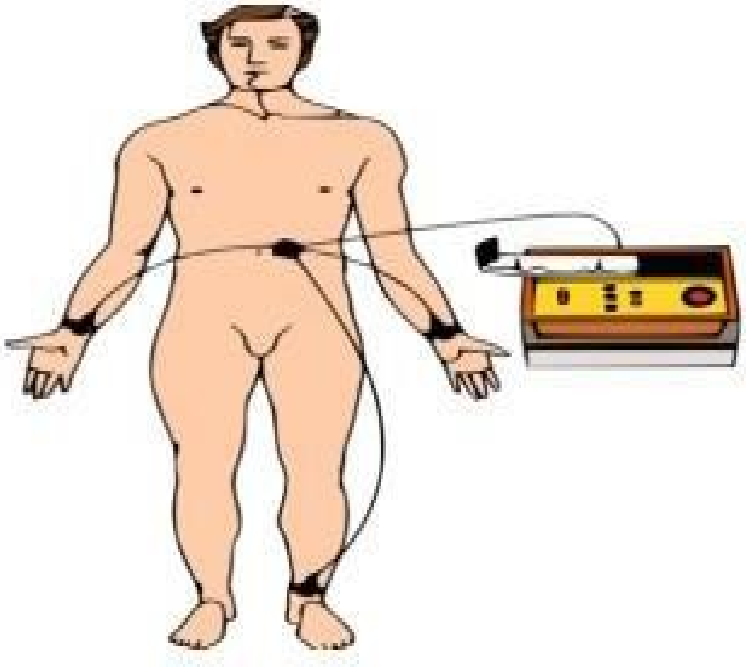

Figure1. Leads placed on the patinet's body.

In order to reduce the electromyogram noise, the signal at the a Vf lead is used as a primary input while the difference of the signals between leads a Vr and a Vl become the input reference .The ECG signals used in this study were selected from the MIT-BIH library from subject with normal, Left Ventricle Event (LVE) and Atrial Fibrillation (AF) conditions, and were corrupted with electromyogram noise. The remainder of the paper is organized as follows. In section II the proposed method is described in detail followed by the results and discussion in section III. Conclusions are provided in section IV.

ECG signal is one of the biomedical signals, which are widely studies and applied in clinic. A normal ECG waveform is usually composed of P wave, QRS complexes, and T wave, and the accurate detection of them is important to analyze ECG signal. However, because ECG signal is very faint, it is extremely easy to interfere by the different noises while gathering and recording. How to suppress noises effectively is always an important problem in the detection of ECG signal.Recently, wavelet transform has been widely used in signal and image processing due to the time-frequency localization characteristics. There are mainly two kinds of wavelet denoising methods used in denoising of ECG signal: one is wavelet transform modulus maxima

method. This method can eliminate noises and remain the information of the original signal in maximum at the same time, but the amount of calculation is great, and the process of calculation may be unstable. The other is wavelet thresholding denoising method. Wavelet thresholding denoising method deals with wavelet coefficients using a suitable threshold chosen in advance. The wavelet coefficients at different scales could be obtained by taking discrete wavelet transform (DWT) of the noisy signal.Normally, those wavelet coefficients with smaller magnitudes than the preset threshold are caused by the noise and replaced by zero, and the others with larger magnitudes than the preset threshold are caused by original signal mainly and kept (hard-thresholding case) or shrunk (the soft-thresholding case). Then the denoised signal could be reconstructed from the resulting wavelet coefficients. This method is simple and easy to be used in denoising of ECG signal. But hard-thresholding denoising method may lead to the
oscillation of the reconstructed ECG signal. The soft-thresholding denoising method may reduce the amplitudes of ECG waveforms, and especially reduce the amplitudes of the R waves. To overcome these disadvantages mentioned above,an improved thresholding denoising method is proposed firstly.It is a compromising method between the hard- and soft-thresholding. Secondly, a new translation-invariant (TI) wavelet denoising method with improved thresholding is presented to eliminate the noise of ECG signal.

The electrocardiogram (ECG) is the recording of the cardiac activity and it is extensively used for diagnosis of heart diseases.It is also an essential tool to allow monitoring patients at home, thereby advancing telemedical applications. Recent contributions in this topic are reported in . Even though these contributions are for different projects, the issue common to each is the use of ECG for remote monitoring and assistance under different telecommunication platforms. The transmission of ECG often introduces noise due to poor channel conditions.Moreover, there are other types of noise inherent in the data collection process. These artifacts are particularly significant during a stress test.

The main sources of such artifacts are:

(1) the baseline wander (BW) mainly caused by respiration, and

(2) high-frequency noise such as the electromyography (EMG)noise caused by the muscle activity. Moreover, the motion of the patient or the leads affects both types of artifacts. In ECG enhancement, the goal is to separate the valid ECG from the undesired artifacts so as to present a signal that allows easy visual interpretation.Many approaches have been reported in the literature to address ECG enhancement. Some recent relevant contributions have proposed solutions using a wide range of different techniques, such as perfect reconstruction maximally decimated filter banks and nonlinear filter banks, advanced averaging, the wavelet transform, adaptive filtering , singular value decomposition , and independent component analysis.

In this paper, we propose a new method for ECG enhancement based on the empirical mode decomposition (EMD).The EMD was recently introduced in as a technique for processing nonlinear and nonstationary signals. It also serves as an alternative to methods such as the wavelet analysis, the Wigner–Ville distribution, and the short-time Fourier transform.It is proposed as a preprocessing stage to efficiently compute the instantaneous frequency through the Hilbert transform ,although it can be applied independently as well.It is reported in that EMD behaves as a "wavelet-like"dyadic filter bank for fractional Gaussian noise. This conclusion has been applied in a detrending and denoising example in .The work in presents one of the first application of EMD in biomedical engineering, where blood pressure is studied.Regarding ECG signal processing, one of the first EMD-based contributions, which investigates the chaotic nature of ECG. Also related to the cardiac system, the EMD is utilized in the analysis of heart rate variability (HRV). The EMD is also used for artifact reduction in gastric signals . Finally, in the EMD is utilized to extract the lower esophagealsphincters pressure in the gastro esophageal reflux disease.As the brief review above demonstrates, the EMD is a good tool for artifact reduction applications. This motivates the proposed use of the EMD for ECG enhancement. In this work, we address both denoising and BW removal based on the EMD.The contributions ofthis work lie in two aspects. First, we introduce the use of the EMD in ECG

enhancement. Second, noting that both high-frequency noise and BW components are mixed with ECG signal component in the EMD domain, we develop novel methods to remove both types of artifacts. The performance of the proposed algorithm is demonstrated through various experiments performed over several records from the MIT–BIH arrhythmia database . Quantitative and qualitative experiments are carried out for synthetic and real noise cases. The experimental studies show that the proposed EMD-based method is a good tool for ECG denoising and BW removal, especially for the important real noise cases.

In neurobiology, one often has to deal with time series data that are nonstationary. Fourier-based methods are only designed for the frequency analysis of stationary time series, and thus have limited use in revealing the underlying neurophysiologic variations in such data. The major drawback of Fourier-based approaches is that the basis functions are fixed, and therefore cannot capture anytime-varying characteristics of neural signals.

In the present analysis, we use a new method, called empirical mode decomposition (EMD), that was first introduced by Huang et al. The decomposition is based on direct extraction of the signal energy associated with various intrinsic time scales. The technique adaptively decomposes nonstationary signals into a set of intrinsic oscillatory modes. The components, called intrinsic mode functions (IMFs), allow the calculation of a meaningful multi-component instantaneous frequency by virtue of the Hilbert transform. Thus, one can potentially localize events in time and frequency. Here, we explore the use of EMD to study neuronal activity in the visual cortical area V4 of macaque monkeys performing a visual spatial attention task. Local field potentials (LFPs) and multiunit activity were simultaneously recorded from multiple V4 sites with overlapping receptive fields (RFs). The monkey fixated a central spot, and after a short delay, two stimuli were presented at equal eccentricity,one inside and one outside the RFs. On separate trials, the monkey was required to attend to the stimulus at one (target) location, and was rewarded for responding when the target changed color, ignoring changes at the other (distracter) location.

Target and distracter color changes were equiprobable and distributed uniformly between 0.5 and 5 s after stimulus onset. The result was two attention conditions:attention inside the RF vs. attention outside the RF. The analysis described here used LFPs from one V4 site on 300 trials correctly performed by a monkey whose attention was directed within the RF of that site.In the sections below, we begin with a brief introduction to the EMD method, then describe the results of its application to V4 LFP data, and finally discuss the neurophysiological processes that it suggests.

1.2 Methods

Huang's data-driven EMD method was initially proposed for the study of oceanwaves, and found immediate applications in biomedical engineering. The major advantage of EMD is that the basis functions are derived directly from the signal itself. Hence the analysis is adaptive, in contrast to Fourier analysis, where the basis functions are fixed sine and cosine waves.

The central idea of this method is an iterative sifting process that decomposes a given signal into a sum of IMFs, those basic building blocks that make up data complex time series. A signal must satisfy two criteria to be an IMF: (1) the number of extrema and the number of zero crossings are either equal or differ at most by one;802 H. Liang et al. / Neurocomputing 65–66 (2005) 801–807and the mean of its upper and lower envelopes equals zero. The first criterion is similar to the narrow-band requirement. The second criterion modifies a global requirement to a local one, and is necessary to ensure that the instantaneous frequency will not have unwanted fluctuations as induced by asymmetric waveforms.To make use of EMD, the signal must have at least two extreme one maximum and one minimum to be successfully decomposed into IMFs.Given these two definitive requirements of an IMF, the sifting process for extracting an IMF from a given signal x(t) is described as follows:

1. Two smooth splines are constructed connecting all the maxima and minima of x(t)to get its upper envelope, xup(t), and its lower envelope, xlow(t); The extrema can be simply found by determining the change of sign of the derivative of the signal.Once the extrema are identified, all the maxima are connected by a cubic spline line as the upper envelope. The procedure is repeated for the local minima to produce the lower envelope. All the data points should be covered by the upper and lower envelopes.

2. The mean of the two envelopes is subtracted from the data to get their difference

$$d(t) = x(t) - (x_{up}(t) + x_{low}(t))/2.$$

3. The process is repeated for d(t) until the resulting signal, c1(t), the first IMF,satisfies the criteria of an intrinsic mode function.The residue

$r_1(t) = x(t) - c_1(t)$ is then treated as new data subject to the sifting process as described above, yielding the second IMF from r1ðtÞ: The procedure continues until either the recovered IMF or the residual data are too small, in the sense that the integrals of their absolute values or the residual data have no turning points. Once all of the wavelike IMFs are subtracted from the data, the final residual component represents the overall trend of the data.At the end of this process, the signal x(t) can be expressed as follows:

$$x(t) = \sum_{j=1}^{N} c_j(t) + r_N(t),$$

where N is the number of IMFs, $r_N(t)$ denotes the final residue (signal trend), and cj(t) are nearly orthogonal to each other, and all have zero means. Due to this iterative procedure, none of the sifted IMFs is derived in closed analytical form.In practice, after a certain number of iterations, the resulting signals do not carry significant physical information, because, if sifting is carried on to an extreme, it could result in a pure frequency modulated signal of constant amplitude. To avoid this, we can stop the sifting process by limiting the standard deviation, computed from two consecutive sifting results, which is usually set between 0.2 and 0.3. By construction, the number of extrema is decreased when going from one residual to the next, and the whole

decomposition is guaranteed to be completed with a finite number of modes.By the sifting process, the data are represented by intrinsic mode functions, to which the Hilbert transform can be applied. The Hilbert spectrum enables us to represent the amplitude and the instantaneous frequency as functions of time in a three-dimensional plot. The resulting time–frequency distribution of the amplitude is called the Hilbert amplitude spectrum. The two-step procedure, EMD and its subsequent Hilbert spectral analysis, is called the Hilbert–Huang transform (HHT). The HHT method provides not only a more precise definition of particular events in time–frequency space than wavelet analysis, but also more physically meaningful interpretations of the underlying dynamic processes.

High-frequency denoising by the EMD is in general carried out by partial signal reconstruction, which is premised on the fact that noise components lie in the first several IMFs. This strategy works well for those signals whose frequency content is clearly distinguished from that of noise and is successfully applied in. The basic idea is to statistically determine the index of the IMFs that contain most of the noise components,beginning from fine to coarse scale. Given the index, the IMFs corresponding to the noise are removed and the reconstruction of the original signal is obtained by summing up the remaining IMFs. However, this approach cannot be assumed in the ECG case because the QRS complex spreads over the lower-order IMFs. Therefore, in the ECG case, EMD-based denoising requires a different strategy.Noise encountered in ECG applications is usually located in the high-frequency band. Although most ECG signal power is concentrated in lower frequencies, the QRS complex spreadsacross the mid- to high-frequency bands. This complicates ECG denoising since lowpass filtering or simply removing lower order IMFs will introduce severe QRS complex distortion, e.g.,R-wave amplitude attenuation. As Section 2 illustrates, the EMD decomposes a signal into IMFs with decreasing frequency content. The EMD of clean and noisy ECG records are illustrated in the following two examples, thus revealing specific patterns associated with the QRS complex and noise in the EMD domain.Consider first a clean ECG signal (first lead of record

103)from the MIT–BIH arrhythmia database decomposed by theEMD as shown in Fig. 1.

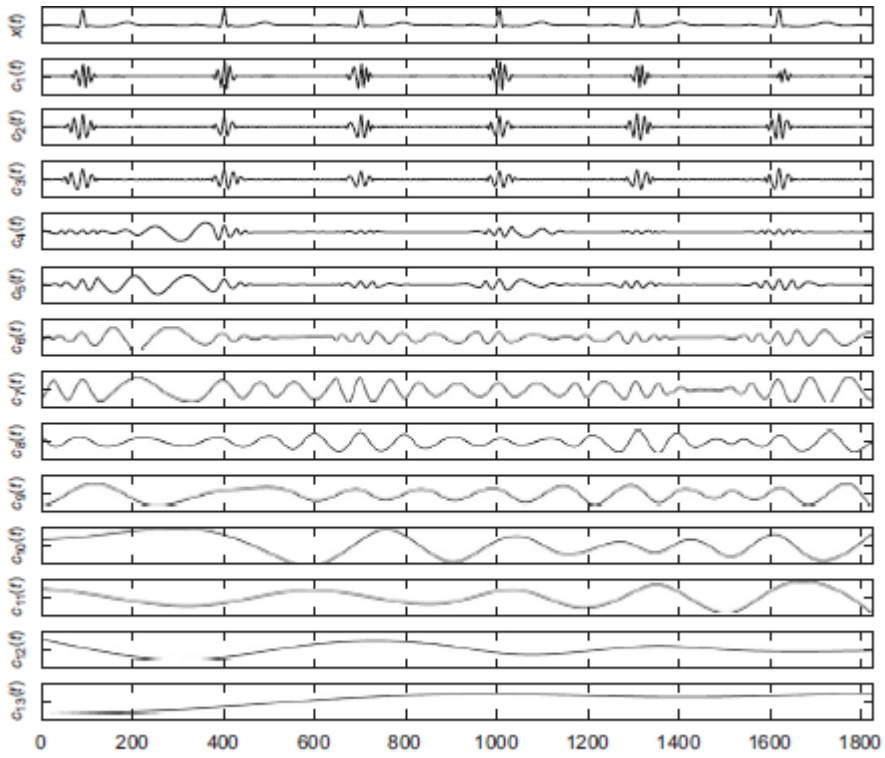

Fig. 1. EMD of a clean ECG. From top to bottom: clean ECG and resulting IMF 1–13. Vertical axes of subplots are not in the same scale.

The top plot shows the original ECG,and the remaining show all the IMFs from low to high orders.As we can see, the frequency content of each individual IMF decreases as the order of IMF increases. Note that the oscillatory patterns observed in the first three IMFs are mainly due to the QRS complex, which has strong high-frequency components.This observation can be used to delineate the QRS complex.Consider next the EMD of a noisy ECG. A representative noisy signal is obtained by adding Gaussian noise to the clean signal in Fig. 1, the result of which is shown in the top graph of Fig. 2. The IMFs of the noisy signal are also shown in Fig. 2.

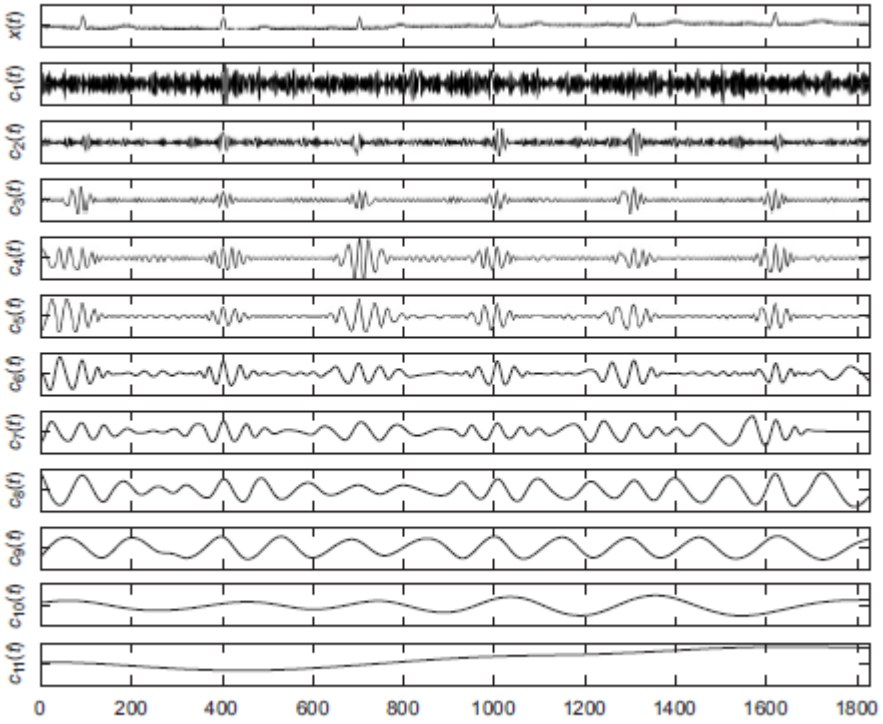

Fig. 2. EMD of a noisy ECG. From top to bottom: noisy ECG and its IMF 1–11. Vertical axes of subplots are not in the same scale.

Compared to the clean signal case, the first IMF of the noisy signal contains strong noise components. The oscillatory patterns of the QRS complex become more apparent starting from the second IMF. An analysis of EMD on clean and noisy ECG indicates that it is possible to filter the noise and at the same time preserve the QRS complex by temporal processing in the EMD domain. Multiple evaluations show these characteristics for all EMD decompositions of ECG signals. Therefore,the following four steps constitute the proposed denoising procedure:

(1) Delineate and separate the QRS complex.
(2) Use proper windowing to preserve the QRS complex.
(3) Use statistical tests to determine the number of IMFs contributing to the noise.
(4) Filter the noise by partial reconstruction.

1.3 Delineation of the QRS complex:

To preserve the QRS complex, we need a delineation of the QRS complex. The oscillatory patterns in the first several IMFs indicate a link between these patterns and the QRS complex.Therefore, the first several IMFs can be jointly used to delineate the QRS complex. Our scheme utilizes the first three IMFs. That is, they are summed together to yield a signal which is used for delineation. Experiments show that this three term partial sum is sufficient to delineate the QRS complex.

The QRS complex and the oscillatory patterns in the first three IMFs are illustrated in the example of Fig. 3 for both clean and noisy ECG signals. In these two figures, the ECG signal is
plotted in a solid line and the dash-dotted line is the sum of the first three IMFs: $d(t)=c1(t)+c2(t)+c3(t)$.A close examination of Fig. 3(a) reveals that the QRS complex is bounded by the two zero-crossing points of $d(t)$. One zero-crossing point is on the left-hand side of the local minimum near the fiducially point(R-wave) and the other is on the right- hand side of the local minimum near the fiducially point, as shown in Fig. 3(a). Even in the noisy case (Fig. 3(b)), this relation holds, which shows that the usage of the three IMFs is a valid choice in the sense that it is less affected by the noise.Given the sum of the first three IMFs $d(t)$, we can delineate the QRS complex through the following procedure: (1) Identify the fiducial points.(2) Apply the EMD to the noisy ECG signal. Sum the first three IMFs to obtain $d(t)$.(3) Find the two nearest local minima on both sides of the fiducial.(4) Detect the two closest zero-crossing points on the left hand side of the left minimum and on the right-hand side of the right minimum. These two points are identified as boundaries of the QRS complex.Here, and in the remainder of the paper, we assume that the fiducial points are either known (for example, by annotation)or can be determined by some other methods.

1.4 Windowing to preserve the QRS complex

Next, a window function is designed to preserve the QRScomplex. The window function is a time domain window applied to the first several IMFs corresponding to the noise. A general design guideline for the QRS preserving window function is that it should be flat over the duration of the QRS complex and decay gradually to zero so that a smooth transition introduces minimal distortion. Since the window size is determined by the delineation results in the first step, these window functions adjust their sizes according to the QRS duration. Atypical window function, and that which is used here, is the Tukey window (tapered cosine window):

$$w(t)=\begin{cases}\frac{1}{2}\left[1+\cos\left(\pi\frac{|t|-\tau_1}{\tau_2-\tau_1}\right)\right], & \tau_1\leqslant|t|\leqslant\tau_2,\\ 1, & |t|<\tau_1,\\ 0, & |t|>\tau_2,\end{cases} \qquad (6)$$

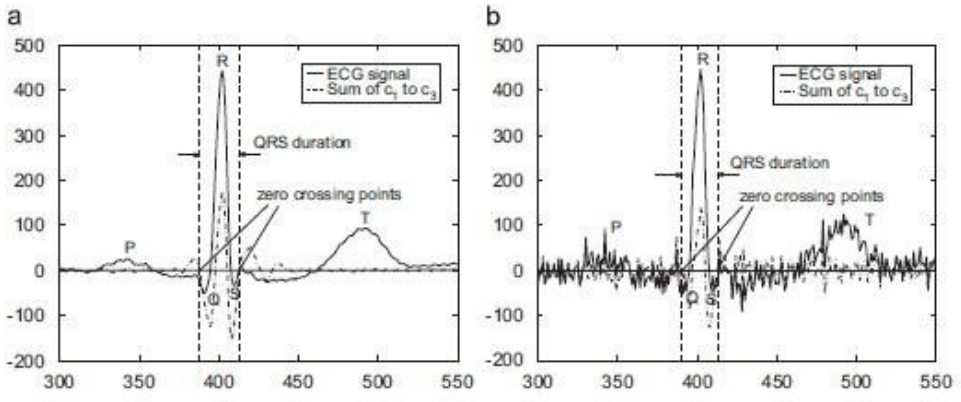

Fig. 3. Delineation of the QRS complex in the EMD domain. The solid line is the ECG signal and the dash-dotted line is the sum of the first three IMFs: $c_1(t)+c_2(t)+c_3(t)$. (a) Clean ECG, (b) noisy ECG.

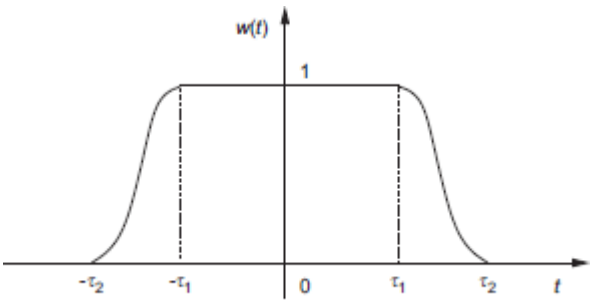

Fig. 4. Tukey window (tapered cosine) function.

whereλ1 is the flat region limit and λ2 is the transition region limit. The graphical representation of the Tukey window is shown in Fig. 4.When using (6), the flat region width 2λ1 is chosen such that it equals the QRS complex boundary determined by the method in Section 3.1. The transition region is set to avoid abrupt "cutoff" of the window and reduce the distortions. As shown in Figs. 1 and 2, the spread of the oscillatory pattern around the QRS complex increases with the IMF order. Consequently,a variable width transition region in (6) is adopted to cope with the spreading effect of the various IMFs. We define the ratio between the one-sided transition region length |λ1−λ2|and the flat region length 2λ1 as

$$\beta = \frac{|\tau_1 - \tau_2|}{2\tau_1}, \qquad (7)$$

where βis a free parameter. For example, for the first IMF,β can be set to be 30%. Likewise, for the jth IMF, β is chosen as $j \times 30\%$, which indicates that the window itself spreads as the QRS complex spreads with increasing order of IMF. The number of the IMFs that are dominated by noise, referred to as the *noise order*, must be established. For ECG signals,the contaminating noise is usually zero mean while the signal is nonzero mean. This fact enables the noise and signal to be separated in the EMD domain. Since lower-order IMFs contain the noise, we perform a statistical test to determine if a particular combination of IMFs has zero mean. An example of such a test is the t -test, which is also used in to identify the noise-contributing IMFs.The t

-test is able to establish if the mean of the IMF deviates from zero. In the *t* -test, we perform the following hypothesis testing:

$$\begin{aligned} &H_0: \quad \text{mean}(c_{PS}^{M}(t)) = 0, \\ &H_1: \quad \text{mean}(c_{PS}^{M}(t)) \neq 0, \end{aligned} \tag{8}$$

where c_{PS}^{M} is the *M*th-order partial sum of the IMFs:

$$c_{PS}^{M}(t) = \sum_{i=1}^{M} c_i(t). \tag{9}$$

By selecting a certain significance level _, the null hypothesisH0 is rejected in favor of the alternative hypothesis H1 if the *p* value is less than _. Thus, starting from the first IMF, we perform a *t* -test on the partial sum *cM*PS*(t)* for *M* = 1, 2, . . .until we obtain a partial sum *cPt*
PS*(t)* that accepts the alternative hypothesis. The IMF order *Pt* at the termination point indicates
that there are *Pt* IMFs that contribute primarily to the noise,and is thus set as the noise order. The role of the noise order in the EMD-based method is similar to the cutoff frequency in frequency domain filtering, and indicates how many IMFs should be removed.In some cases the ECG itself has a mean close to zero. Using the previous technique to determine the noise order in such cases results in over smoothing or loss of information since the noise order will be very large. To avoid this potential problem,the noise order is set as

$$P = \min(P_t, 5), \tag{10}$$

Where *Pt* is the noise order obtained from the *t* -test. The rationale for (10) is that IMFs with order higher than five typically contain little or no noise. Thus, this approach avoids the over smoothing problem without sacrificing noise removal.*3.4. Denoising by partial reconstruction*
Having established a method to determine the noise order,we can filter the noise by partial IMF reconstruction. To preserve the QRS complex, the

window functions are applied to the *P* IMFs considered to be noise components. For the *i*th IMF, a window function $\psi_i(t)$ is constructed by concatenating the window functions (6), each of which centered at the QRS complex is applied. Mathematically,

$$\psi_i(t) = \sum_{j=1}^{N_r} w_{ij}(t), \tag{11}$$

Where *Nr* is the number of QRS complex and *wij (t)* denotes the variable size window for the *j*th QRS complex in the *i*th IMF.The aim of the window function $\psi_i(t)$ is to eliminate the noise and retain the QRS complex. To further reduce the distortion,we define the complementary window function which is given by

$$\bar{\psi}_i(t) = 1 - \psi_i(t), \quad \forall t. \tag{12}$$

Clearly, $\bar{\psi}_i(t)$ suppresses the QRS complex and retains some noise information. Its effect is contrary to that of . Here, is applied to the $\psi_i(t)$ $\bar{\psi}_i(t)$ first *P* IMFs in conjunction with $\bar{\psi}_i(t)$.The main reason of using the complementary window function is to avoid abrupt changes to the QRS complex by allowing a negligible amount of noise components in the lower-order IMFs. The sum of the *P* windowed IMFs, the remaining *N –P*IMFs, and the residue forms the reconstructed signal:

.

$$\hat{x}(t) = \sum_{i=1}^{P} \psi_i(t) c_i(t) + \sum_{i=1}^{P} a_i \bar{\psi}_i(t) c_i(t) + \sum_{i-P+1}^{N} c_i(t) + r_N(t), \tag{13}$$

where $0<ai<1$ is the attenuation coefficient. Typically *ai* can be chosen between 0.1 and 0.3.

1.5 ECG BW removal using EMD:

Since BW is a low-frequency phenomenon, it is expected that the major BW components are located in the higher-order IMFs. The residue, which can also be regarded as the last IMF,may not correspond to the BW because the BW may have multiple extrema and zero crossings, which violates the residue definition. Indeed, the BW spreads over the last several IMFs.Simply removing the last several IMFs may introduce significant distortions. Thus, the BW must be separated from the desired components in the last several IMFs. Moreover, as in the denoising case, the number of IMFs that contribute to the BW must be established. This number is referred to as BW *order*.To remove the BW, a BW estimate is first obtained via a "multiband" filtering approach. The estimated BW is then subtracted from the signal, yielding the reconstructed signal. A bank of lowpass filters are applied to the last several IMFs. The sum of the output of this filter bank serves as the BW estimate.Suppose the signal with BW is *x(t)*. After performing the EMD, we obtain all the IMFs:

$$x(t) = \sum_{i=1}^{N+1} c_i(t), \qquad (14)$$

where the residue is included in the summation as the last IMF,$cN+1(t)$. Denote the BW order as Q. We design a bank of lowpass filters $hi\ (t\ ),\ i = 1, 2, \ldots, Q$, and then filter the IMFs starting from the last, $cN+1(t)$, by these lowpass filters. The outputs of these filters are

$$\begin{aligned} b_1(t) &= h_1(t) * c_{N+1}(t), \\ b_2(t) &= h_2(t) * c_N(t), \\ &\vdots \\ b_Q(t) &= h_Q(t) * c_{N-Q+2}(t), \end{aligned} \qquad (15)$$

where∗ denotes the convolution. The cutoff frequencies of the lowpass filters are chosen as follows. Set the cutoff frequency of the first lowpass filter *h*1*(t)* to be ω_o. The cutoff frequency of the *k*th filter is set as

$$\omega_k = \frac{\omega_0}{M^{k-1}}, \qquad (16)$$

Where $M>1$ is a frequency-folding number. The cutoff frequencies are related in this fashion due to the fact that, as the IMF order decreases, fewer BW components, but more signal components, are present in the IMF. This multiband filtering scheme considers each IMF as a subband of the signal and performs filtering on each subband. The output *bi (t)* extracts the BW component in each IMF. Therefore, it can be used to determine the BW order *Q*. The variance of each *bi (t)* is determined as

$$\text{var}\{b_i(t)\} = \frac{1}{L-1}\sum_{t=0}^{L-1}[b_i(t) - \mu_{b_i}]^2, \qquad (17)$$

Where μ*bi* is the mean value of *bi (t)*. Starting from the last IMF ,we choose *Q* such that var{*bQ*+1*(t)*}<*ξ* and var{*bQ(t)*}>=ξ ,where ξis an appropriate established threshold. The selection of the parameters, ω_o.,*M,ξ,* can be based on *a priori* knowledge or can be experimentally tuned according to the BW behavior. In the later simulations, some typical values are given for these parameters.

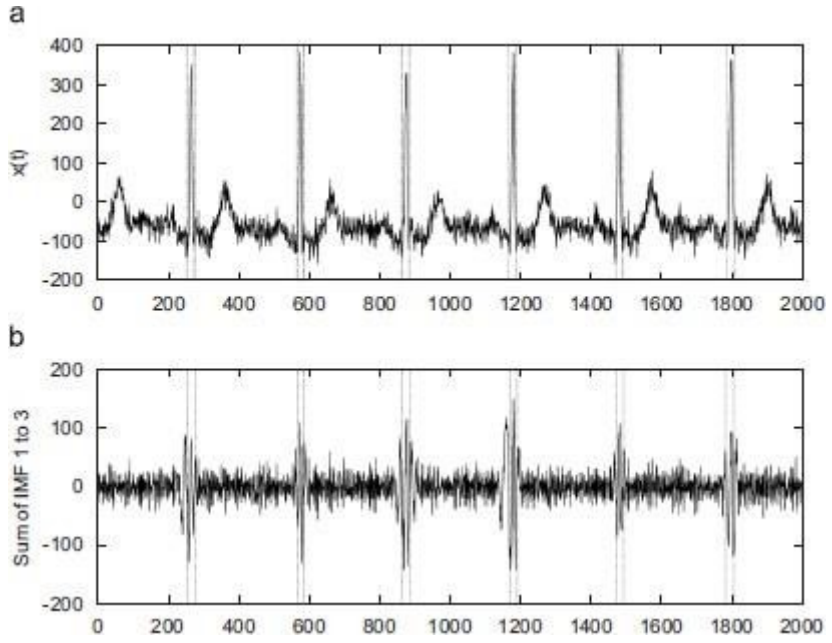

Fig. 2. QRS complex delineation results. The delineated boundaries are shown in dashed lines. (a) Noisy signal, (b) correspondence in the sum ofthe first three IMFs.

Once the BW order Q is determined, the outputs of all the filters are synthesized to form the estimate

$$\hat{b}(t) = \sum_{i=1}^{Q} b_i(t). \tag{18}$$

Finally, removing the BW yields the reconstructed signal

$$\bar{x}(t) = x(t) - \hat{b}(t). \tag{19}$$

In the most general case, ECG signals are contaminated by both high-frequency noise and BW. The method of denoising in Section 3 and the method of removing BW in Section 4can be combined to remove both artifacts. Because the noise only affects the lower-order IMFs while the BW only affects the higher-order IMFs, the methods do not interfere with each

other. Consequently, the reconstructed signal after removing both high-frequency noise and BW is

$$\hat{x}(t) = \sum_{i=1}^{P} \psi_i(t) c_i(t) + \sum_{i=1}^{P} a_i \bar{\psi}_i(t) c_i(t) + \sum_{i=P+1}^{N+1} c_i(t) - \sum_{j=1}^{Q} h_j(t) * c_{N-j+2}(t), \quad (20)$$

where the residue *rN(t)* in (13) is rewritten as *cN*+1*(t)*.

CHAPTER 2

ELECTROCARDIOGRAPHY

Electrocardiography is the interpretation of electrical activity of the heart over a period of time, which produces a representation of ECG. The ECG is a crucial diagnostic tool in clinical practice. It is especially useful in diagnosing rhythm disturbances, changes in electrical conduction, and myocardial ischemia and infarction. In noninvasive electrocardiography, the signal is detected by electrodes attached to the outer surface of the skin and recorded by a device external to the body. The sections of this chapter describe the methods used for recording Electrocardiograms. The locals of electrodes and the respective signal associated to those locals. Then will be presented a brief exposition about the instrumentation used in ECG field.

2.1 Methods for Recording Electrocardiograms

The ECG is recorded by placing an array of electrodes at specific locations on the body surface. This is possible because the heart is suspended in a conductive medium. Figure 3.1 shows the ventricular muscle within the chest. When one portion of the ventricles depolarizes and therefore becomes negative with respect to the remainder parts of the heart, forming a potential difference. The electrical currents flow from the depolarized area to the polarized area in large circuitous routes.
It is this electrical field that can be collected under surface of the heart. In fact, this is the summation of all action potentials mentioned in section 2.3.

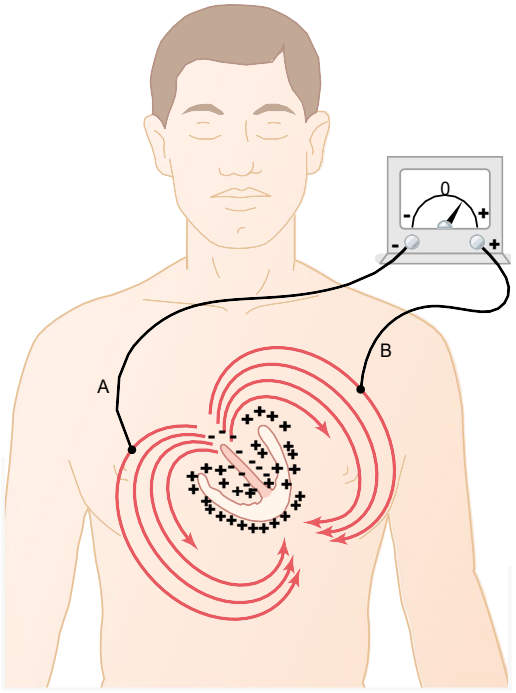

Figure 2.1: *Flow of current in the chest around partially depolarized ventricles.*

2.1.1 Electrocardiographic Leads

Conventionally, electrodes are placed on each arm and leg, and six electrodes are placed at defined locations on the chest. Three basic types of ECG leads are recorded by these set of electrodes: standard bipolar limb leads, chest leads and augmented limb leads. The limb leads are referred as bipolar leads because each lead uses a single pair of positive and negative electrodes. The augmented leads and chest leads are unipolar leads because they have a single positive electrode with other electrodes coupled together electrically to serve as a common negative electrode.

Figure 2.2 shows electrical connections between the patient limbs and the electrocardiograph for recording electrocardiograms from the so-called standard bipolar limb leads. In these arrangements the electrocardiogram is recorded from two electrodes located on different sides of the heart, in this case, on the limbs. Three different connections are possible, Lead I, Lead II and Lead III.

Lead I In recording limb Lead I, the negative terminal of the electrocardiograph is connected to the right arm and the positive terminal to the left arm. Therefore,

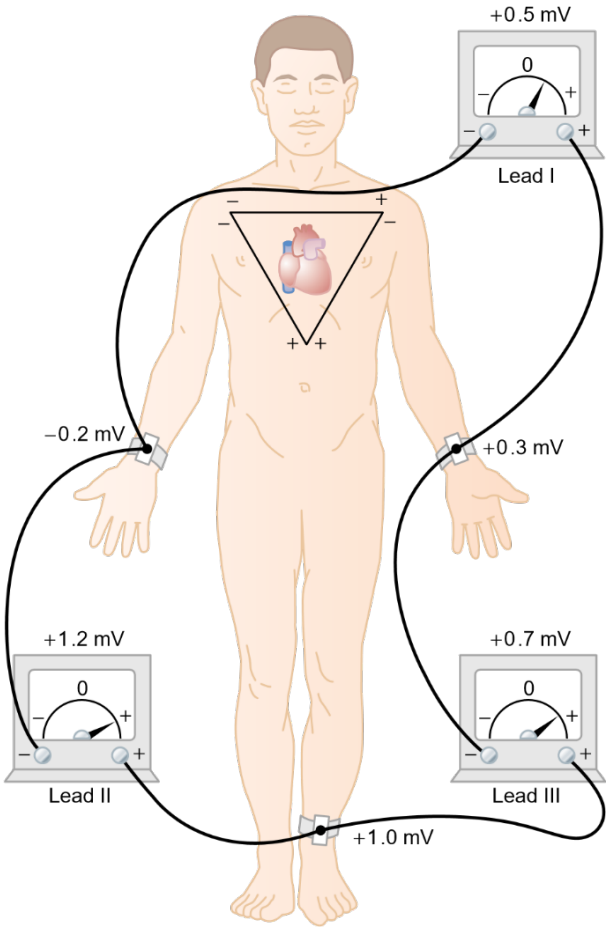

Figure 2.2: *Conventional arrangement of electrodes for recording the standard electrocardiographic leads. Einthoven's triangle is superimposed on the chest[6].*

the electrode of the right arm is electronegative with respect to the electrode of the left arm. The electrocardiograph records a positive signal, that is, above the zero voltage reference line in the electrocardiogram. When the opposite is true, the electrocardiograph records below this line.

Lead II To record limb lead II, the negative terminal of the electrocardiograph is connected to the right arm and the positive terminal to

the left leg. Therefore, when the right arm is negative with respect to the left leg, the electrocardiograph records positively.

Lead III To record limb lead III, the negative terminal of the electrocardiograph is connected to the left arm and the positive terminal to the left leg. This means that the electrocardiograph records a positive signal when the left arm is negative with respect to the left leg.

These three limb leads roughly form an equilateral triangle with the heart at the

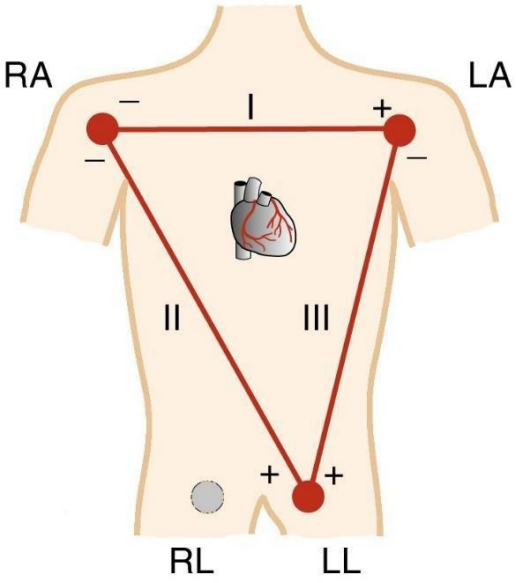

Figure 2.3: *Einthoven Triangle with the placement of the standard ECG limb leads and the location of the positive and negative recording electrodes for each of the three leads. RA, right arm; LA, left arm; RL, right leg; LL, left leg*

center, refer to Figure 2.3. This triangle is called Einthoven's triangle in respect of Willem Einthoven who developed the ECG in 1901. The two vertices at the upper part of the triangle represent the points at which the two arms are electrically connected, and the lower vertex is the electrode located on the right leg used as a ground point.

Depending on the lead used to record the ECG signal, the resultant shape is slightly different, this differences can be observed in Figure 2.4.

In the three electrocardiograms represented in Figure 2.4, it can be seen, that at any given instant the sum of the potentials in leads I and III equals the potential in lead II, thus illustrating the validity of Einthoven's law.

The signals from these leads are identical between them, it does not matter greatly which lead is recorded when one wants to diagnose different cardiac arrhythmias, because diagnosis of arrhythmias depends mainly on the time relations between the different waves of the cardiac cycle.

2.1.METHODS FOR RECORDING ELECTROCARDIOGRAMS

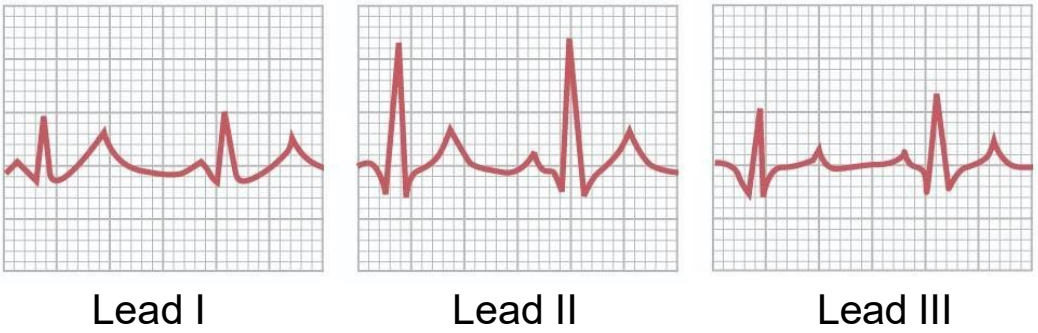

Figure 2.4: *Normal electrocardiograms recorded from the three standard electrocardiographic leads.*

Chest Leads

When it is important to diagnose damages in the ventricular or atrial muscles, or in the Purkinje conducting system, the three Bipolar Limb Leads records are not useful. For these cases, we need leads that can show the abnormalities of cardiac muscle contraction or cardiac impulse conduction in these areas. The preferred leads for diagnose these cases are the chest leads, also called Precordial Leads, which are represented in Figure 3.5. These leads are used to record ECG with one electrode placed on the anterior surface of the chest directly over the heart at one of the points shown in Figure 2.5. The different recordings are known as leads V_1, V_2, V_3, V_4, V_5, and V_6. This electrode is connected to the positive terminal of the electrocardiograph, and the negative electrode, called the indifferent electrode, is connected through equal electrical resistances to the right arm, left arm, and left leg, all at the same time. Usually these six standard chest leads are recorded, one at a time, where the chest electrode is being placed sequentially at the six points shown in the figure.

Figure 3.6 illustrates the electrocardiograms of the healthy heart as recorded from these six standard chest leads. Each chest lead records mainly the

electrical potential of the cardiac musculature immediately beneath the electrode, because the heart surfaces are close to the chest wall. Therefore, relatively minute abnormalities in the ventricles, particularly in the anterior ventricular wall, can cause marked changes in the electrocardiograms recorded from individual chest leads.

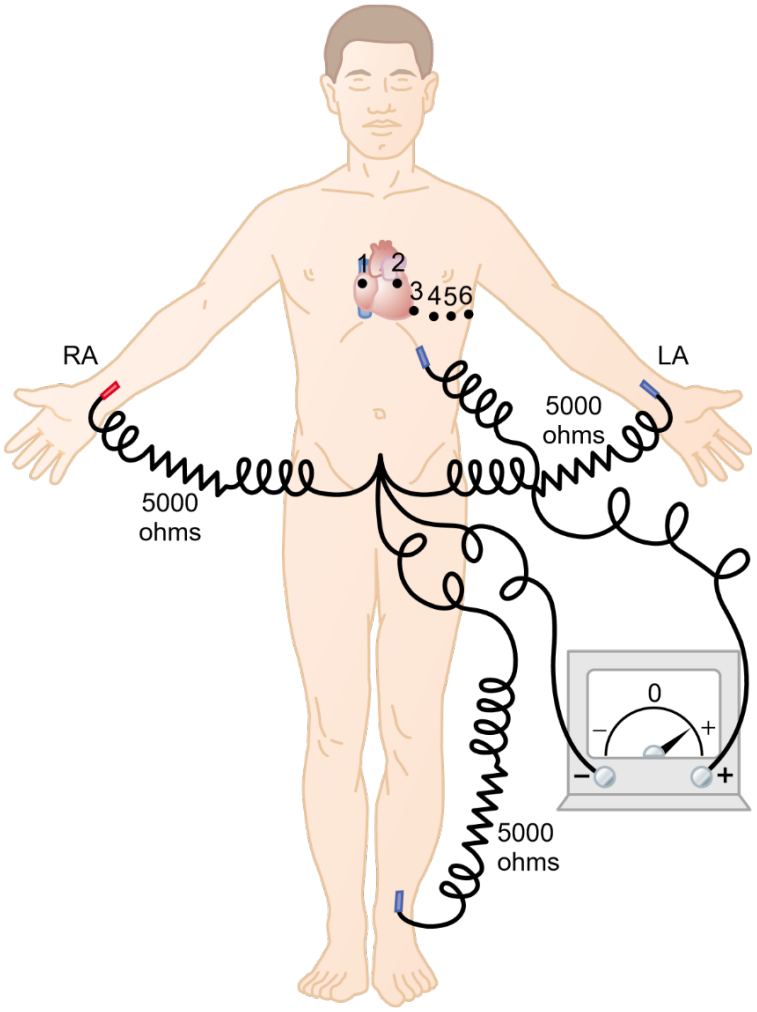

Figure 2.5: *Connections of the body with the electrocardiograph for recording chest leads. LA, left arm; RA, right arm.*

Augmented Unipolar Limb Leads

Another system of leads in wide use is the augmented unipolar limb lead. In this type of recording, two of the limbs are connected through electrical resistances to the negative terminal of the electrocardiograph, and the third limb is connected to the positive terminal. When the positive terminal is on the right arm, the lead is known as the aVR lead; when on the left arm, the aVL lead; and when on the left leg, the aVF lead. Figure 3.7 showns the angular position of these leads in respect to bipolar limb leads. The normal

recordings of this arrangement are shown in Figure 2.8. They are all similar to the standard limb lead recordings, except that the recording from the aVR lead is inverted due to the polarity connections to the electrocardiograph.

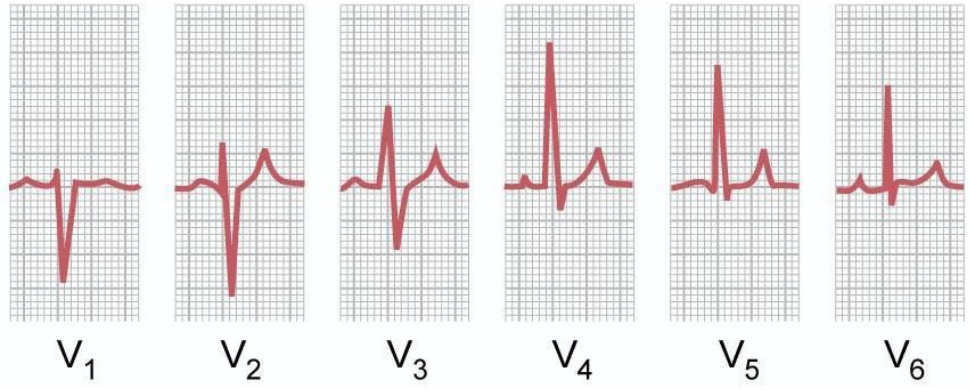

Figure 2.6: *Normal electrocardiograms recorded from the six standard chest leads.*

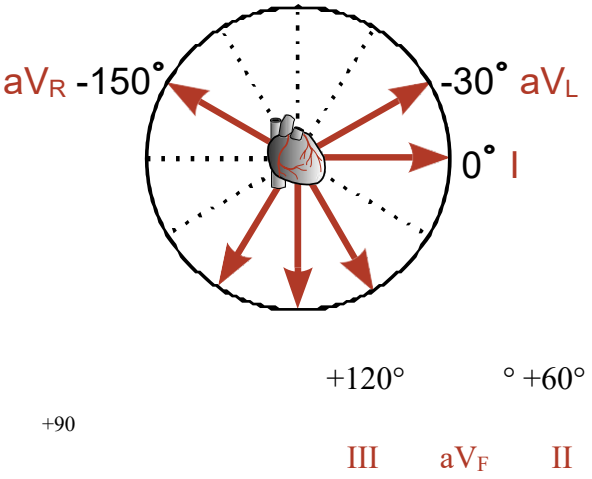

Figure 2.7: *The angular position of Augmented Unipolar Limb Leads in respect to Bipolar Limb Leads.*

2.2 ECG Instrumentation

The electrical activity of the heart is fairly simple to measure. In the very early 1900s, Willem Einthoven won the Nobel Prize in medicine for his work identifying and recording the parts of the electrocardiogram. Figure 3.9b) shows a photography of Willem Einthoven and Figure 3.9a) a photography of its complete electrocardiograph machine with a patient. Today's medical instruments are considerably more complicated and diverse, mainly because they incorporate electronic systems for sense, manipulate, store, and display data and information. Today, an electrocardiograph is more compact and offers several functionalities, *e.g.* the model PageWriter

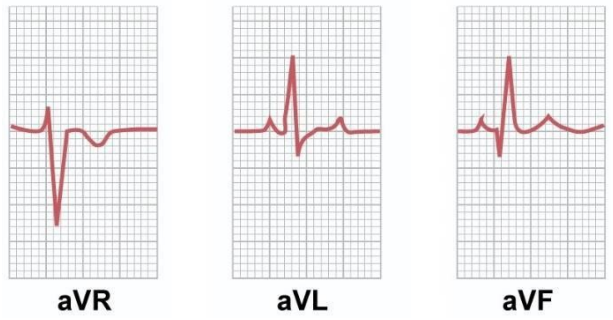

Figure 2.8: *Normal electrocardiograms recorded from the three augmented unipolar limb leads.*

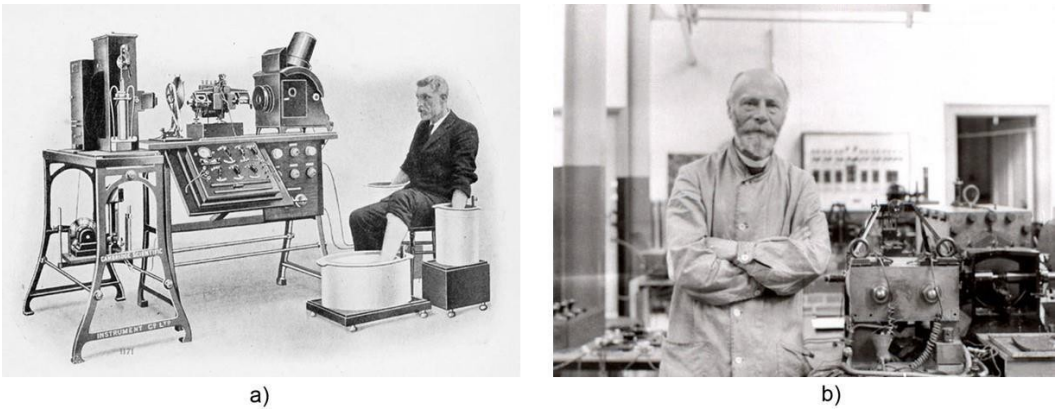

Figure 2.9: *a) Photograph of a complete electrocardiograph, showing the manner in which the electrodes are attached to patient, in this case the hands and one foot being immersed in jars of salt solution. b) Willem Einthoven in the lab.*

TC70 from Philips shown in Figure 3.10a) offers the possibility to record 20 minutes of up to 16 leads simultaneously, into a box of 40 x 33 x 16 cm. In Figure 3.10b) it is shown the model StressVue from same supplier used for stress ECG recordings, for example during an exercise.

Mostly of these equipments are considered High Resolution ECG (HRECG) systems, where at least three bipolar leads are used in an anatomic *xyz* coordinate system.

2.2.1 The Ambulatory ECG

Due to their complexity, medical ECG equipments are used mostly in hospitals and medical centres by trained personnel, but some also can be found in private homes operated by patients themselves or their caregivers. Examples of these equipments are the portable devices for personal usage and long term recorders called Holter

Figure 2.10: *a) Philips electrocardiograph model PageWriter TC70. b) Philips stress testing system StressVue.*

devices. The original large-scale clinical use of this technology was to identify patients who developed heart block transiently and could be treated by implanting a cardiac pacemaker. The very first device was developed by Dr. Norman Jeff Holter in the early 1940s, refer to Figure 3.11a), where the data is recorded into a tape and the weight of this equipment surrounds 38 Kg, Figure 3.11b) shows a patient holding the Holter monitor[11]. The evolution of Holter ECG is closely followed by technical

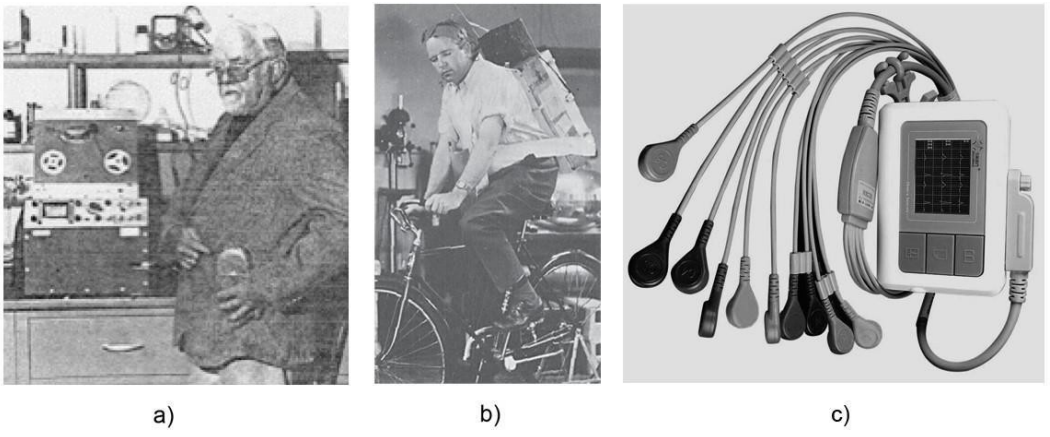

Figure 2.11: *a) Dr. Norman Jeff Holter (1914-1983) with original Holter; b) A patient with the original Holter device from 1947; c) Low cost modern Holter model MIC-12H-3L from Beijing Jinco Medical.*

and clinical progress. A modern Holter device can record tree to twelve simultaneous leads from 24 to 48 hours into a digital memory. Figure 3.11c) shows an example of a low cost modern Holter model MIC-12H-3L from Beijing Jinco Medical, with ability to record twelve leads during 24 hours.

2.2.2 Electrocardiograph Block diagram

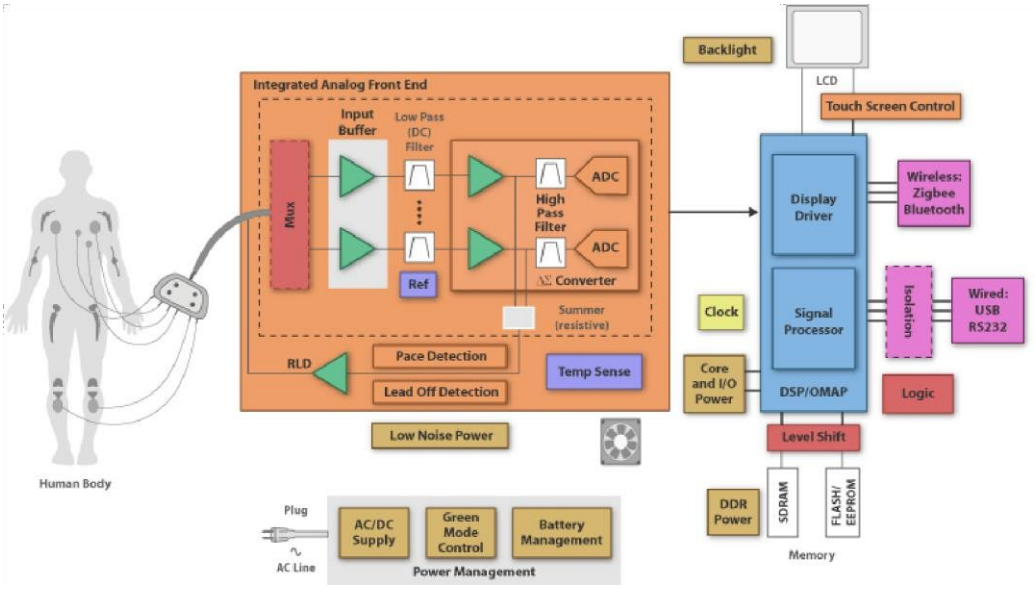

Figure 2.12: *ECG system block diagram.*

Figure 2.12 shows the block diagram of an ECG system. Basic functions of an ECG machine include: ECG waveform display, either through Liquid Crystal Display (LCD) screen or printed paper media, and heart rhythm indication as well as simple user interface through buttons. More features, such as patient record storage through convenient media, wireless/wired transfer and 2D/3D display on large LCD screen with touch screen capabilities, are required in more and more ECG products. Multiple levels of diagnostic capabilities are also assisting doctors and people without specific ECG trainings to understand ECG patterns and their indication of a certain heart condition. After the ECG signal is captured and digitized, it will be sent for display and analysis, which involves further signal processing.

2.3 ECG Electrods

The measurements of electrical activity in the heart, muscles, or brain are examples of direct measurements of physiological energy. For these measurements, the energy is already electrical and only needs to be converted from ionic to electronic current using an electrode. To collect ECG at surface of skin, it is indispensable the use of electrodes, and the electrodes used by non-evasive electrocardiography are so many that will be only covered here their principal aspects.

The electric characteristics of bio-potential electrodes are generally nonlinear and a function of the current density at their surface. But electrodes are usually represented by linear models due to they operation at low potentials and currents. Under these conditions, electrodes and the skin model can be represented by the equivalentcircuit shown in Figure 3.13. In this circuit R_P and C_P are components

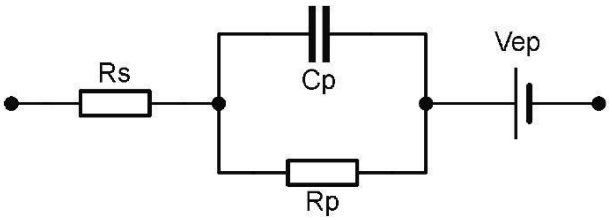

Figure 2.13: *Liner model of an electrical equivalent circuit for a bio-potential electrode.*

that represent the impedance associated with the electrode-electrolyte interface and polarization at this interface. R_s is the series resistance associated with interfacial effects and the resistance of the electrode materials themselves, and V_{ep} represents the half-cell potential. Half-cell potential is associated to the distribution of ions or charged molecules in a biologic structure. The half-cell potential occurs due to the interaction between the metal of the electrode and the solution used near to the metal surface. The use of this solution is crucial for better adapting the contact between the electrodes and the skin. In fact, when the cations in this solution and the metal of the electrodes are the same, the half-cell potential is reduced. The values of these potentials are dependent of the characteristics of materials and can be described by the Nernst:

$$V_{ep} = -\frac{GT}{nF} \ln Q \qquad (3.1)$$

Where T is the absolute temperature (Kelvin), $G = 8.31451 Jmol^{-1}K^{-1}$) is the idealgas constant, $F = 96485.3 Cmol^{-1}$ is Faraday's constant, and n is the number or electrons transferred in the balanced oxidation/reduction reaction, and Q is the reaction quotient, *i.e.* the extracellular and intracellular concentrations.

V_{ep} value is the value corresponding to materials/reactions $Ag{+}Cl^{-} \rightarrow AgCl{+}e^{-} = +0.223V$. This constant is based on the assumption that electrode distance between metal and skin is constant. If this distance changes V_{ep} take much higher values, which is described as motion artefacts[1]. The most important aspect is that the presence of the electrode does not affect the variable being measured.

Depending on the type of ECG that are being measured, different electrodes

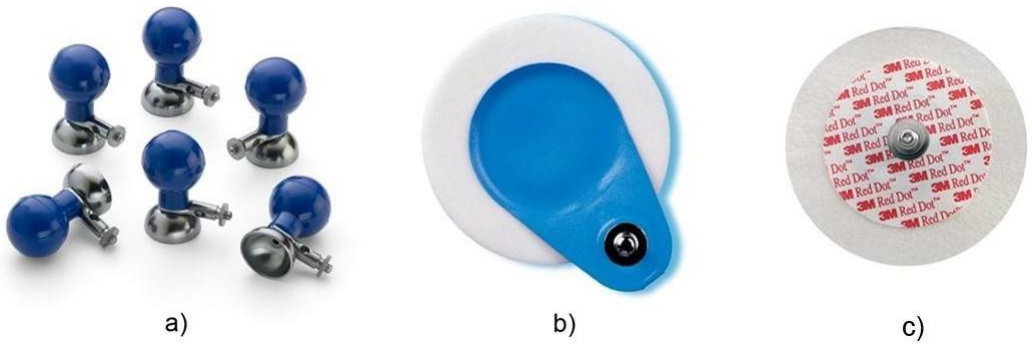

Figure 2.14: *ECG electrodes: a) electrodes for diagnostic resting, b) electrodes for stress test and Holter, c) electrodes for monitoring.*

should be used. In the market it is possible to find different types of electrodes, but they mainly occupy three different families: electrodes for diagnostic resting ECG, Figure 2.14a); electrodes for stress test and Holter ECG, Figure 2.14b); electrodesfor monitoring ECG, Figure 2.14c).

CHAPTER 4

NOISE

Noise is present in almost all environments, and can be defined as an undesirable signal that interferes with the desired signal. A noise itself is a signal that can be generated from several sources, and takes different spectrum distributions. In fact, biomedical electrical signals, which are the scope of this work, are always polluted with some kind of noise. These interference signals includes interferences from power supplies, motion artefacts due to patient movement, radio frequency interference, defibrillation pulses, pace maker pulses, interferences from other monitoring equipment, etc. The big chall4enge of noise in biomedical signals is closely related with amplitude of the desired signals face to the noise, *i.e.* the Signal-to-Noise Ratio (SNR). For instance, an ECG measurement gets challenging due to the presence of the large DC offset and various interference signals. This potential can be up to 300 mV for a typical electrode, which is several times larger than ECG signal. Noise reduction is an important task to solve in biomedical signals and for this reason, the understanding of noise characteristics is the focus of the contents in this chapter. The chapter will starts with noise properties and characteristics as SNR and separability, followed by most common noises sources associated to ECG. Finally it is presented the literature review about the methodologies used to ECG signal denoising.

4.1 Noise Properties

Depending on its frequency or time characteristics, a noise process can be classified in several categories: Narrowband noise, White noise, Band-limited white noise, Coloured noise, Impulsive noise and Transient noise pulses. Narrowband noise is a noise process with a narrow bandwidth such as a 50Hz hum from the power lines. White noise is purely random noise that has a flat power spectrum. White noise theoretically contains all frequencies in equal intensity. Band-limited white noise it is a noise with flat spectrum and limited bandwidth that usually covers the limited spectrum of the device or the signal of interest. Coloured noise it is nonwhitenoise or any wideband noise whose spectrum has a non-flat shape; examples are pink noise, brown noise and autoregressive noise. Impulsive noise consists of short-

duration pulses of random amplitude and random duration. And transient noise pulses consists of relatively long duration noise pulses.

4.1.1 Noise Characteristics

Noise is usually represented as a random variable, $x(n)$, and describing his properties as a function of time it is not very useful. Therefore, it is more common the evaluation of its probability distribution, range of variability, or frequency characteristics.
While noise can take a variety of different probability distributions, the *Central Limit Theorem*[2] implies that noises will have a Gaussian or normal distribution. The probability $p(x)$ of a Gaussianly distributed variable, x, is specified by the normal or Gaussian distribution equation:

$$p(x) = \frac{1}{\sigma\sqrt{2\pi}} e^{\frac{-(x-a)^2}{2\sigma^2}} \tag{4.1}$$

Where, a it is the *mean*, or average value, and σ^2 is the *variance*. The arithmetic quantities of mean and variance are frequently used in signal processing algorithms. The mean value of a discrete array of N samples is evaluated as:

$$\overline{x} = \frac{1}{N} \sum_{k=1}^{N} x_k \tag{4.2}$$

And the variance, σ^2, is calculated as:

$$\sigma^2 = \frac{1}{N-1} \sum_{k=1}^{N} (x_k - \overline{x})^2 \tag{4.3}$$

From Equation (4.3) we grasp the standard deviation σ, which is just the square root of the variance.
Normalizing Equation (4.3) by:

$$\frac{1}{N-1} \tag{4.4}$$

will produces the best estimate of the variance if x is a sample from a Gaussian distribution. Alternatively, normalizing the Equation (4.3) by:

$$\frac{1}{N} \tag{4.5}$$

produces the second moment of the data around x, which is equivalent to RMS value of the data if the data have zero as mean value.

If noise is captured from different sensors, such as sensor array, or multiple observations from the same source, the standard deviation of noise becomes reduced by the square root of the number of averages.

4.1.2 Signal-to-Noise Ratio

From previous notes at beginning of this chapter, signal and noise are relative terms: general speaking, signal is the waveform of interest while noise is everything else. The relative amount of signal and noise present in a waveform is usually quantified by the SNR. As the name implies, this is simply the ratio of signal to noise, both measured in Root-Mean-Squared (RMS) amplitude. The SNR is often expressed in decibel (dB) where:

$$SNR = 20log\frac{Signal}{Noise} \tag{4.6}$$

To convert from dB scale to a linear scale:

$$SNR_{linear} = 10^{\frac{dB}{20}} \tag{4.7}$$

For example, a ratio of 20 dB means that the RMS value of the signal was 10 times the RMS value of the noise, because $10^{20/20} = 10$. A common value in this area is +3 dB, which indicates a ratio of $10^{3/20} = 1.414$, and -3 dB means that the ratio is 1/1.414. If noise and signal has the same amount in RMS value, this means 0 dB. As an example, Figure 4.1 shows an ECG signal with different amounts of white noise. Notice that it is very difficult to detect presence of ECG signal visually when the SNR is -3 dB, and impossible when the SNR is -10 dB.

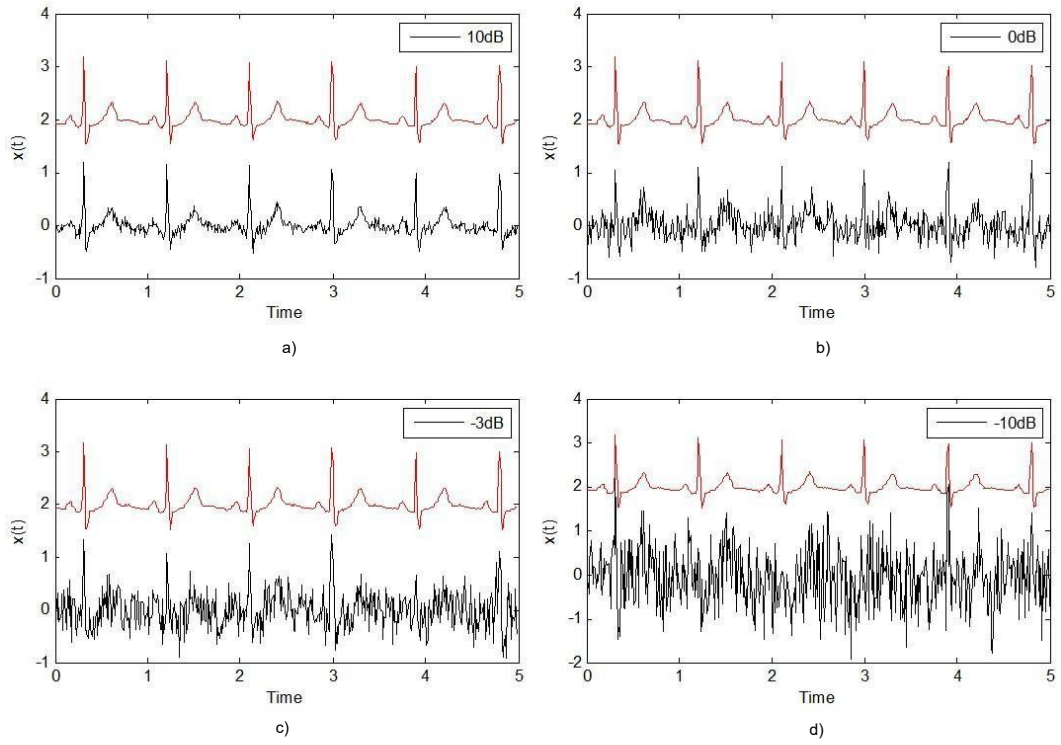

Figure 4.1: *A ECG signal with varying amounts of added noise. The signal is barely discernable when the SNR is -3 dB and not visible when the SNR is -10 dB.*

4.1.3 Separability of Signal and Noise

A signal is completely recoverable from noise if the spectra of the signal and the noise do not overlap. An example of a noisy signal with separable signal and noise spectra is shown in Figure 4.2(a). In this case, the signal and noise are placed in different parts of the frequency spectrum, and signal can be denoised with a lowpass filter. Although, Figure 4.2(b) illustrates a more common example of signal and noise, with overlapping spectra. For these cases, it is not possible to completely separate the signal from the noise; however, the effects of the noise can be more or less reduced depending on the filter technique used.

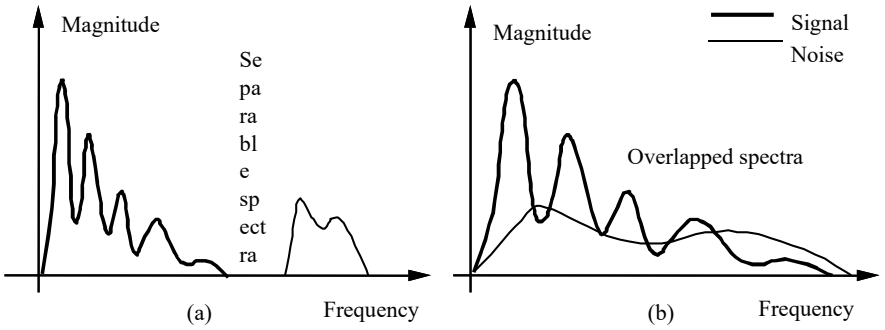

Figure 4.2: *Illustration of separability: (a) The signal and noise spectra do not overlap, and the signal can be recovered by a low-pass filter; (b) the signal and noise spectra overlap, and the noise can be reduced but not completely removed.*

4.1.4 Noise Correlation

A important aspect that should be taken into account is how well one instantaneous value of noise correlates with the adjacent instantaneous values, *i.e.* how muchone data point is correlated with its neighbours. Correlation is a statistical measurement of the relationship between two variables. The values of correlation are in a range of +1 to −1, where zero correlation means that there is no relationship between the variables; −1 means a perfect negative correlation; and +1 indicates a perfect positive correlation. Perfect negative correlation is when one variable goes up the other goes down, and perfect positive correlation is when both variables move in the same direction together. For complete random noise with flat distributions, the correlation is zero, and in practice, most electronic sources produce noise that is essentially white up to many megahertz. But, after filtering process, it becomes band limited which is commonly referred as coloured noise[3]. Coloured noise shows correlation between adjacent points, this correlation becomes much stronger as the bandwidth goes to more monochromatic.
Correlation is a very important aspect to keep in mind when applying the adapting filter techniques discussed in Chapter 5.

4.2 Noise Sources

The presence of noise is fulfilled in various degrees in almost all environments. The most known and common are:*Acoustic Noise*, that emanates from moving, vibrating, or colliding sources and is the most familiar type of noise present in everyday environments; *Electromagnetic Noise*, wich is present at all frequencies and in particular at radio frequencies; *Processing Noise*, that results from the signal

processing, *e.g.* quantisation noise in digital coding, or lost data packets in digital data communication systems.

4.2.1 Biomedical Noises Sources

Noise frequently is a limitation factor in the performance of medical instrumentation, producing variability. In biomedical measurements, variability has four different origins:

1. Physiological variability;
2. Transducer artifact;
3. Environmental noise or interference;
4. Electronic noise.

Physiological Variability Physiological variability is due to the presence of other sources of biological influences than those of interest. For example, assessment of respiratory function based on the measurement of blood pO_2[4] could be confounded with other physiological mechanisms that change blood pO_2. Physiological variability can be a very difficult problem to solve, where to solve it, sometimes it is required information provided by different sources to help in validation.

Transducer Artefact Transducer artefact is produced when the transducer is the responsible to change the desired signal. For example, non-invasive recordings of electrical potentials using electrodes placed on the skin are sensitive to motion artefact.

Environmental Noise Environmental noise is generated from existing sources, either external or internal to the body. For example, in a fetal ECG recording, the fetal ECG is corrupted by the mother ECG. In these cases it is not possible to describe the specific characteristics of environmental noise.

Electronic Noise Electronic noise falls into two broad classes: thermal or Johnson noise[5], and shot noise. The former is produced primarily in resistor or resistance materials while the latter is related to voltage barriers associated with semiconductors. Both sources produce noise with a broad range of frequencies often extending from DC to $10^{12} - 10^{13}$Hz.

4.3 ECG Noises Sources

ECG signals always have background noise associated, and noise sources are so many that noise reduction became an important frontend signal processing task for biomedical signals. The most common noises that usually should be considered are: Power line interference, muscular contraction (EMG), Instrumentation noise generated by electronic devices, Baseline drift and ECG amplitude modulation. Power line interference is a narrow-band noise centred at 50 Hz with a bandwidth of less than 1 Hz. This type of noise usually contains harmonics due to parasite currents through human body. Power line interference is relatively constant during the ECG measurement. Cables used in electrodes connections are another source of power line noise.

Muscular contractions produce artefacts within millivolts level potentials. This signal is normally transient bursts of zero mean band-limited Gaussian noise. The worst case of muscular contractions interference is when the measurements are made at same time as muscular activity, *i.e.*, in sports or jobs with intense body activity. In these cases, the muscular amplitude signal can completely overlaps the ECG signals. Without muscular activity the noise produced can be negligible due to its insignificant amplitude.

Artefacts generated by electronic devices can produce several different interferences, conducing to unpredictable noise shapes, leading to complete signal distortion or equipment saturation. If they do not consider these situations, these artefacts could be considered similar to Gaussian noise.

Baseline drift and ECG amplitude modulation with respiration occurs during the breathing cycle. The amplitude of ECG signal varies mainly influenced by relative distance between heart and electrodes. This distance is increased when lungs fill and reduces at time of lungs become empty. The effect can be observed as a slow modulation of the ECG amplitude with same frequency as the breathing cycle. The amplitude of the ECG signal also varies by about 15% with respiration.

In addition, physiological and environmental noise affects the ECG power spectrum. ECG power spectrum can provide useful information about heart condition, and if ECG signal is polluted with noise for overall spectrum, becomes difficult to aim this information with good accuracy. Figure 4.3 summarizes the relative power spectra of the ECG, QRS complexes, P and T waves, motion artefact, and muscle noise. This graph reveals that the ECG signal has their energy mainly concentrated in frequencies below than 25 Hz, where the QRS complex assumes the major area. Also

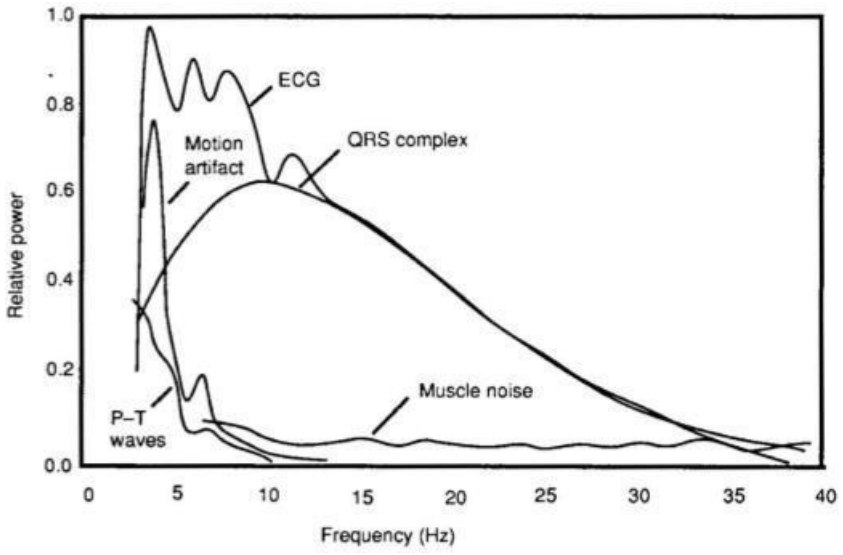

Figure 4.3: *Relative power spectrum of QRS complex, P and T waves, muscle noise and motion artefacts based on an average of 150 beats.*

shows that motion artefact overlapping a small part of ECG signal, and the EMG noise overlaps the entire ECG signal. It is clear that EMG noise can completely destroy ECG in a presence of low SNR.

4.4 ECG Noise Cancelation Techniques

Noise cancellation requires different strategies for different noise sources or types. Since the focus of this paper is a non classical method, the approaches covered in this section are all included in the non-classical methods used by several authors. An useful method for removing power line and baseline disturbances is the application of a digital linear phase filtering. This method can be used to reduce signal magnitude spectrum while preserving the signal time domain as much as possible. The disadvantage of this method is the computational requirements. This is mainly caused by linear phase narrow-band filtering, that requires a long impulse response, and the corresponding number of filter coefficients caused by a large number of multiplications involved in the time domain.

Random and stationary noise can be removed using a temporal averaging method. Noise reduction by temporal averaging method is proportional to the square root of the number of frames or beats taken into the average. This method only offers effective performance if a large number of samples is used. Moreover, due to heartbeats variability, it can cause considerable errors, producing distorted results, or extremely smooth waves.

To increase signal quality, some authors refer the performance of spatial averaging. But spatial averaging requires a large number of electrodes in the same region, which cause the main drawback of the method for portable equipment. This not only causes a discomfort to the users, as well as an amount of signals to be recorded

and treated. Meanwhile, solutions like wearable sensors might be the answer to discomfort, but at time these solutions produces high noise levels due to a bad contact of electrodes at skin surface producing high levels of noise.

To remove muscle noise artifacts in exercise ECG's, Joseph Suresh proposed the SVD (Singular Value Decomposition) method. For a satisfactory performance, SVD filtering do not requires prior information about the onset or offset points of ECG signal, nor knowledge of heartbeat intervals. This is very important since in the presence of a noisy ECG signal it wouldn't be possible to grasp the right position of the wave. SVD method is based on matrix factorization, and the problem of this technique is the matrix dimension and computational calculations before a possible reduction of the matrix. However, mentioned that with a minimum value of matrix size, the results performance of the MSE (mean square error) are identical to the results of the Wiener filter MSE using a discrete cosine transform.

One promising solution for noise reduction is the use of adaptive filters. There are several advantages for adaptive filtering approaches: adapting filtering do not needs a priori knowledge of the statistical or spectral properties of the signal and noise; constantly adapt the weights of filter for better performance; when applied to a set of samples does not require higher power computation requirements. For some applications, the drawback of adaptive filtering approach is that requires the correlation of noise with signal. For the case of ECG, this is not a problem due to the possibility to obtain this correlation from the electro in the leg. Several authors have done their works in this field of signal processing, but mainly with ECG signals from databases as MIT-BIH.

CHAPTER 5

PROPOSED METHOD

Fig. 5.1 shows the structure of a length *L* based adaptive filter with an inputsequence x(n) and with weights updated according to:

$$w(n+1) = w(n) + \mu\, x(n)e(n) \qquad (1)$$

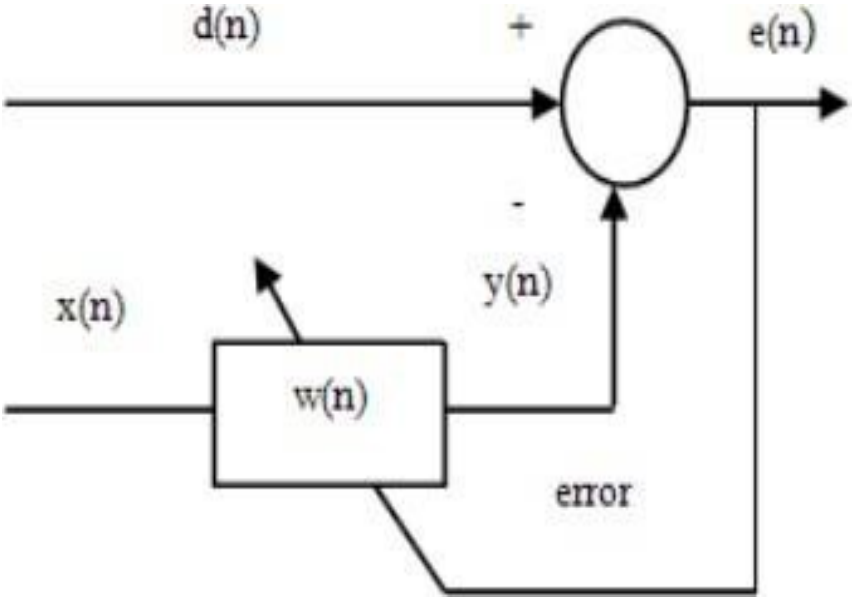

Figure5.1. Adaptive filter structure.

The desired signal, d(n) is a combination of a signal s(n) which is corrupted with a noise signal, and applied to the adaptive filter shown in Fig. 2. The filter error shows as

$$e(n) = x(n) - d(n) \qquad (2)$$

The normalizing step size parameter of the normalized LMS (NLMS) algorithm, results in an improvement of the stability and convergence rate of the filter output compared to the basic LMS adaptive filter . The weight update related to the NLMS algorithm is given by:

$$w(n+1) = w(n) + \frac{\mu\, x(n)e(n)}{x^T(n)x(n)} \qquad (3)$$

where the $x^T(n)x(n)$ is the normalized signal input while μ is a fixed convergence factor to control maladjustment. The proportionate normalized least-mean-square (PNLMS) algorithm has the capability to converge faster than the normalized least mean squares (NLMS) algorithm . Here, the gain has been adapted to the filter at each tap position. The gain is approximately proportional at each position to the current tap weight. The PNLMS algorithm of the weight updated with the extra step-size update G(n+1) is :

$$w(n+1) = w(n) + \frac{\mu\, x(n)e(n)G(n+1)}{x^T G(n+1)x(n)} \qquad (4)$$

and the diagonal matrix of the gain is :

$$G(n+1) = diag[g_1(n+1), \cdots + g_L(n+1)] \quad (5)$$

The gain can be estimated as :

$$g_l(n+1) = \frac{\gamma_l(n+1)}{\frac{1}{L}\sum_{i+1}^{L}\gamma_l(n+1)}, with\ l = 1, \dots, L \quad (6)$$

with the current impulse response as :

$$\gamma_l(n+1) = max[\gamma_{min}(n+1), |\widehat{w}_l(n)|] \qquad (7)$$

And

$$\gamma_{min}(n+1) = \rho\, max\left[\delta_p, |\widehat{w}_1(n)|, |\cdots|, |\widehat{w}_L(n)|\right] \quad (8)$$

where parameters ρ and δp have typical values of 5/L and 0.01, respectively. δp is a small positive number used to avoid overflow. The constant δp become crucial at the moment all coefficients are 0 (at the beginning) and, together with to avoid the very small coefficient to be extinct. The initial convergence become slow down when ρ and δp is too large.

The performance of the PNLMS algorithm becomes inferior to the NLMS algorithm when the current impulse response is scattered. Benesty and Gay proposed an improved version of PNLMS (IPNLMS) algorithm to overcome the disadvantages inherent in the PNLMS algorithm. The IPNLMS algorithm employs a combination of proportionate (PNLMS) and non-proportionate (NLMS) updating technique. The weight updating algorithm and diagonal matrix which related for IPNLMS is sameas (4) and (5) respectively. However, the estimated gain for IPNLMS given by is

$$g_l(n+1) = \frac{1-\alpha}{2L} + (1+\alpha)\frac{|w_l(n)|}{2|\sum_l^0 w_l(n)|}, \quad l = 0,1,\dots,L-1 \qquad (9)$$

The updating algorithm is controlled by a factor of α .It is noted that when α=-1 the second term in (9) becomes zero and thus behaves as a conventional NLMS algorithm. While for α is unity, the first term in goes to zero and as a result it behaves as PNLMS. Deng and Doroslovacki in their study proposed to overcome the slow convergence during PNLMS. An additional μ law to PNLMS (MPNLMS) algorithm is performed, with better results than the PNLMS algorithm. Here, lowering the computational burden on PNLMS may reduce the computational complexity inherent in the PNLMS algorithm and increase the converge performance. The same procedure as (4) and (5) are used by MPNLMS in updating the weight and for diagonal matrix, respectively. A μ law has been added to the PNLMS algorithm with

$$F(|\hat{w}_l(n)|) = \frac{\ln(1+\alpha|\hat{w}_l(n)|)}{\ln(1+\alpha)}, |\hat{w}_l(n)| \ll 1,$$

$$l = 1,\dots,L; \quad \alpha = \frac{1}{\varepsilon} \qquad (10)$$

and change the current impulse response of PNLMS in (8) to

$$\gamma_{min}(n+1) = \rho\, max\left[\delta_p, F|\hat{w}_1(n)|, |\cdots|, F|\hat{w}_L(n)|\right] \qquad (11)$$

and the gain is estimated based on (9) . The constant 1 used in (10) is to avoid negative infinity at the initial stage when w(n+1). The denominator ln(1+α) normalizes the F(|ẃ$_l$(n)|) to be in the range of 0 to 1. The variable ε is a small positive number chosen based on the EMG noise level. The ε is choose based on the Signal to Noise Ratio (SNR) of each signal.

CHAPTER 6

EXPERIMENT RESULTS

Normal, LVE and AF signals taken from the MIT-BIH database were extracted and corrupted by EMG noise as shown in Figure 3 Four different adaptive filters (NLMS) were used to filter the EMG noise contaminated ECG signals.

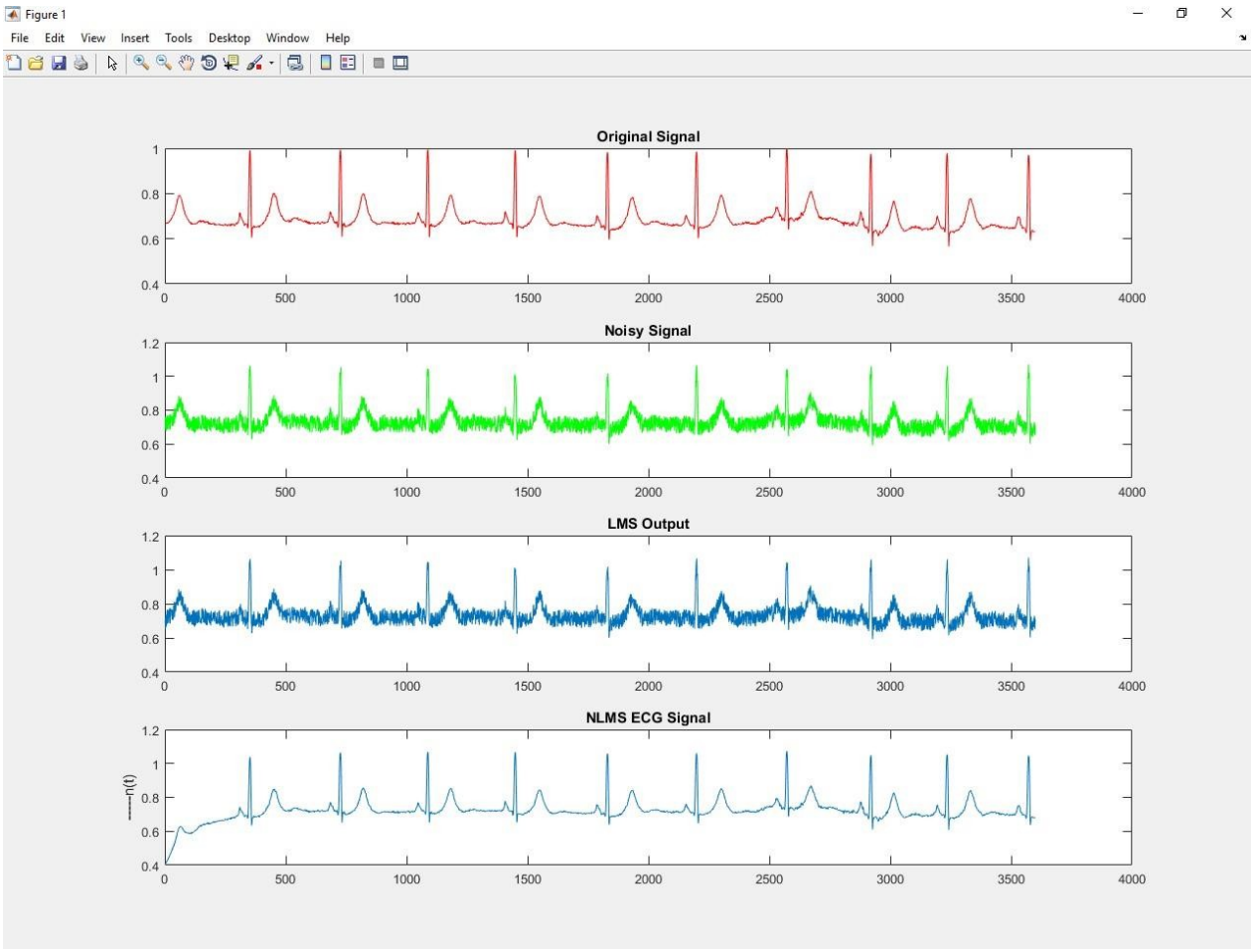

6.1 Final Outputs

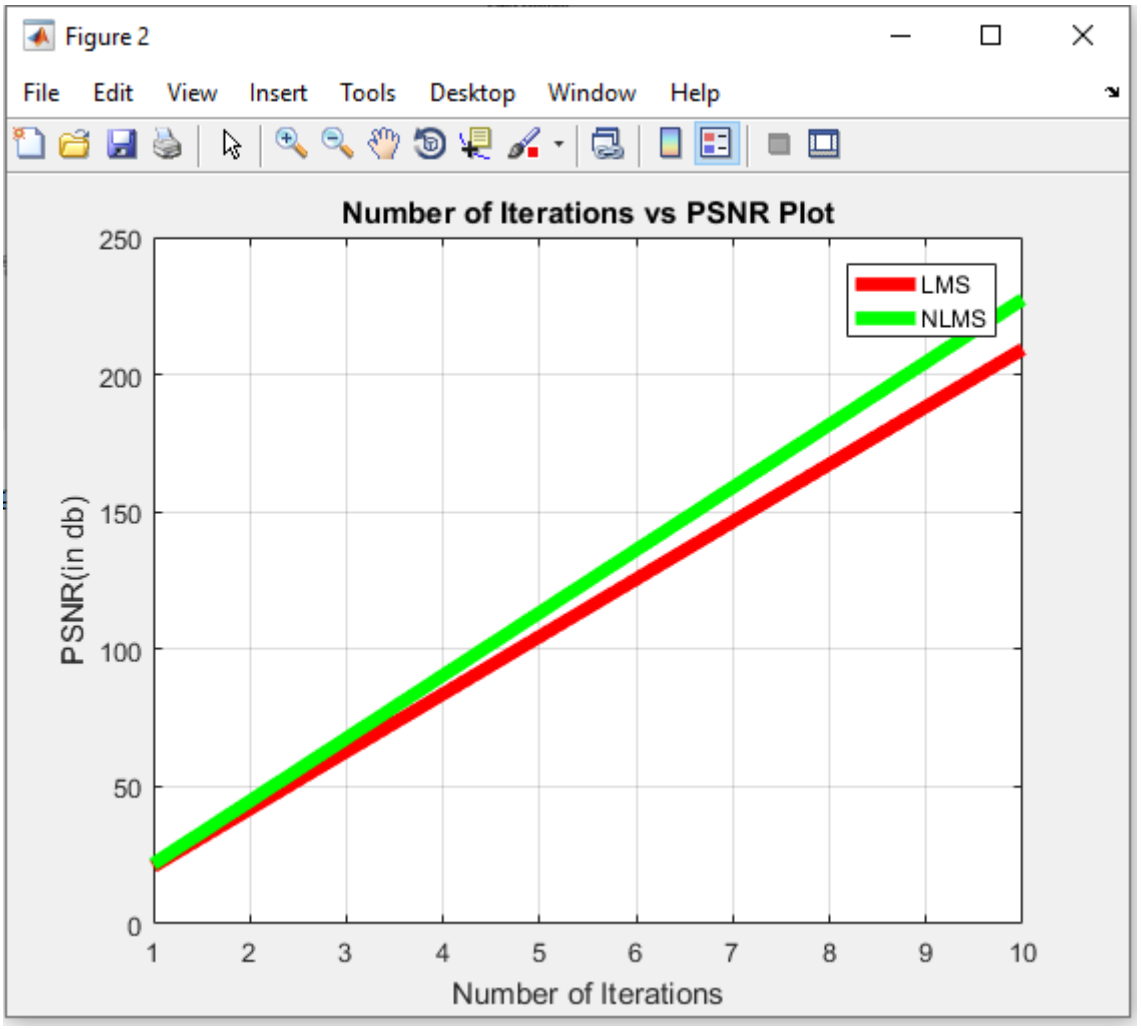

Fig.6.2 PSNR vs Number of Iteration

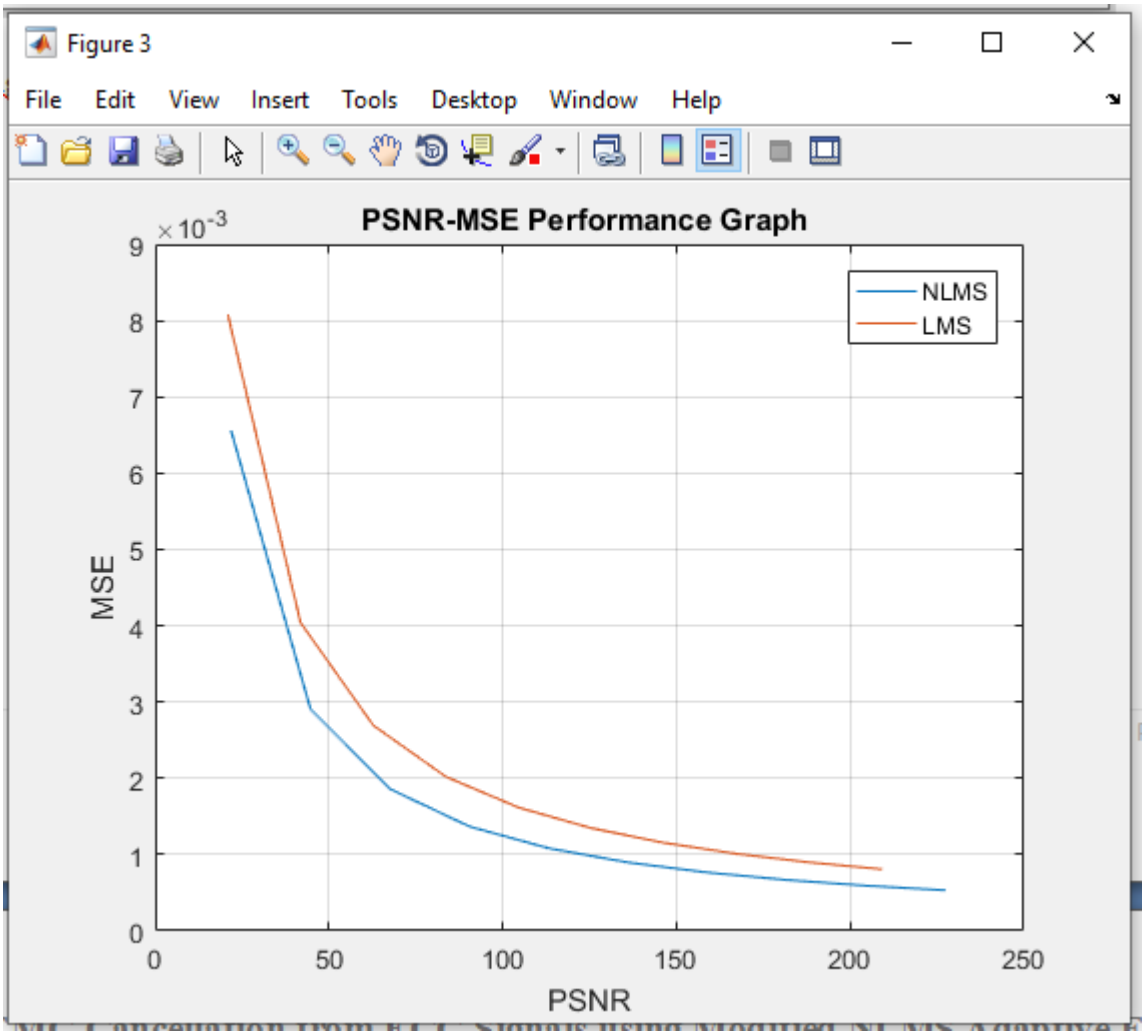

Fig.6.3 PSNR Vs MSE plot

CHAPTER 7
CONCLUSION

The modified NLMS-based adaptive filters are able to produce superior results in reducing EMG noise from the ECG signals of subjects with normal, LVE and AF conditions compared to the conventional NLMS adaptive filter. Compared to the other filters in this study IPNLMS is able to produce the best overall results. The outputs show the capability of the proposed method to reduce the effect of EMG noise and leave behind the important information from the original signal. The modified adaptive filters which are used extensively in the communication fields were shown to be capable of mitigating the effects of ECG signals that are contaminated with EMG noise.

REFERENCES

[1] M. Z. U. Rahman, R. A. Shaik and D. V. R. K. Reddy, "An Efficient Noise Cancellation Technique to remove noise from the ECG Signal using Normalized signed Regressor LMS Algorithm," IEEE International Conference on Bioinformatics and Biomedicine,.

[2] N. V. Thakor and Y. S. Zhu, "Applications of Adaptive Filtering to ECG Analysis: Noise Cancellation and Arrhythmia Detection," IEEE Transactions on Biomedical Engineering, vol. 38(8), pp. 785-794, 1991.

[3] D. G. E. Robertson, G. E. Caldwell, J. Hamill, G. Kamen and S. N. Whittlesey, "Research Methods in Biomechanics". Champaign, Illinois, Human Kinetics Publisher, 2004.

[4] D. A. Tong, K. A. Bartels and K. S. Honeyager, "Adaptive Reduction of Motion Artifact in The Electrocardiogram," Proceedings of Second Joint EMBS/BMES Conference Houston, 2002.

[5] H. Deng and M. Doroslovacki, "Improving Convergence of the PNLMS Algorithm for Sparse Impulse Respose Identification," IEEE Signal Processing Letters, Vol 12(3), 2005.

[6] S. Ohta, Y. Kajikawa and Y. Nomura, "Acoustic Echo Cancellation using Sub-Adaptive Filter," IEEE International Conference on Acoustics, Speech and Signal Processing, 2007. ICASSP 2007.

[7] B. B. Nair, V. P. Mohandas, N. R. Sakthivel, S. Nagendran, A. Nareash, R. Nishanth, S. Ramkumar and D. Manoj Kumar, "Application of Hybrid Adaptive Filters for Stock Market Prediction," International Conference on Communication and Computational Intelligent (INCOCCI), 2010.

[8] S. Selvan, and R. Srinivasan, "Removal of Ocular Artifacts from EEG using an Efficient neural network Based Adaptive Filtering Technique", IEEE Signal Processing Letters, Vol. 6(12), 1999.

[9] S. Mehrkanoon, M. Moghavveyemi and H. Fariborzi, "Real Time Ocular and Facial Muscle Artifacts Removal from EEG Signals using LMS Adaptive Algorithm", International Conference on Intelligent and Advance Systems, 2007.

[10] M. Z. U. Rahman, D. V. R. K. Reddy and Y. Sanggetha, “Staionary and Non-Stationary Noise Removal form Cardiac Signals using a Constrained Stability Least Mean Square Algorithm,” International Conference on Communications and Signal Processing (ICCSP), 2011.

[11] E. Braunwald, “Heart Disease: A Textbook of Cardiovascular Medicine”, Fifth Edition, Philadelphia: WB Saunders Co, 1997. ISBN: 0721656668.

[12] S. Haykin, Adaptive Filter Theory.,Prentice Hall, 2002.

[13] D. L. Duttweiler, “Proportionate Normalized Least Mean Squares Adaptation in Echo Cancelers”, IEEE Transactions on Speech and Audio Processing, Vol. 8(5), pp. 508-518, 2000.

[14] J. Benesty and S. L. Gay, “An Improved PNLMS Algorithm”, IEEE International Conference on Acoustic, Speech and Signal Processing, Vol. 2, pp 1881-1884, 2002.

APPENDIX

MATLAB

Introduction

MATLAB is a high-performance language for technical computing. It integrates computation, visualization, and programming in an easy-to-use environment where problems and solutions are expressed in familiar mathematical notation. MATLAB stands for matrix laboratory, and was written originally to provide easy access to matrix software developed by LINPACK (linear system package) and EISPACK (Eigen system package) projects. MATLAB is therefore built on a foundation of sophisticated matrix software in which the basic element is array that does not require pre dimensioning which to solve many technical computing problems, especially those with matrix and vector formulations, in a fraction of time.

MATLAB features a family of applications specific solutions called toolboxes. Very important to most users of MATLAB, toolboxes allow learning and applying specialized technology. These are comprehensive collections of MATLAB functions (M-files) that extend the MATLAB environment to solve particular classes of problems. Areas in which toolboxes are available include signal processing, control system, neural networks, fuzzy logic, wavelets, simulation and many others.

Typical uses of MATLAB include: Math and computation, Algorithm development, Data acquisition, Modeling, simulation, prototyping, Data analysis, exploration, visualization, Scientific and engineering graphics, Application development, including graphical user interface building.

APPENDIX

SOURCE CODE

1.FREQUENCY ANALYSIS PLOT CODE

```
function
helperFrequencyAnalysisPlot1(F,Ymag,Yangle,NFFT,ttlMag,ttlPhase)
% Plot helper function for the FrequencyAnalysisExample

% Copyright 2012 The MathWorks, Inc.

figure
subplot(2,1,1)
plot(F(1:NFFT/2)/1e3,20*log10(Ymag(1:NFFT/2)));
if nargin > 4 && ~isempty(ttlMag)
  tstr = {'Magnitude response of the ECG signal',ttlMag};
else
  tstr = {'Magnitude response of the ECG signal'};
end
title(tstr)
xlabel('Frequency in kHz')
ylabel('dB')
grid on;
axis tight
subplot(2,1,2)
plot(F(1:NFFT/2)/1e3,Yangle(1:NFFT/2));
if nargin > 5
  tstr = {'Phase response of the ECG signal',ttlPhase};
```

```
else
  tstr = {'Phase response of the ECG signal'};
end
title(tstr)
xlabel('Frequency in kHz')
ylabel('radians')
grid on;
axis tight
suptitle('Frequency Domain analysis of ECG data')
```

2. LMS CODE

```
function [out e]=lms(x,d);
N=length(x);
mu=0.5;
%_____________________
%------ start of the algorithm
w=zeros(1,N-1)';
w(1)=rand(1);
for i=1:N-1
    e(i)=d(i)-w(i)'*x(i);
    w(i+1)=w(i)+mu*e(i)*x(i);
end
out=w(:).*x(:);
```

3. NLMS CODE

```
function [ out1 er ] = nlms(x2,d );
N=length(x2);
mu=.01;
%_____________________
%------ start of the algorithm ========
w=zeros(1,N-1)';
w(1)=rand(1);
p=0.1;
for i=1:N-1
    er(i)=d(i)-w(i)'*x2(i);
    w(i+1)=w(i)+(mu*er(i)*x2(i))./(p+(x2(i)'*x2(i)));
end
% for i=2:N
%     dx(i)=sig1(i)-sig1(i-1);
%     e(i)=d(i)-w(i-1)'*dx(i);
%     de(i)=e(i)-e(i-1);
%     w(i)=w(i-1)+mu*((dx(i)*de(i))/(p+dx(i)^2));
% end

out1=w(:).*x2(:);
```

4.Smoothing CODE

```
function y=smoothing1(PrePulse,N)%   (PrePulse)

% The (2N+1)-Mean smoothing function
% N points smoothing: see line 28(deflaut is 9 points smoothing)
%   input
```

```
%       |__________the first input parameter is the pulse to be smoothed;
%     |__________the second input parameter is the points to be smoothed;
%
%
%
%   output
%         |_________the pulse data after being smoothed by N points



%notice this function the variant of number=size(pulse1,2)
%
number==========size(pulse1,2)
% PrePulse=pulse;                  %// it is used when debugging the function
of smoothing itself.


if (nargin==0)
   disp(' You forget input the signal will be processed and the method of
Wavelet! Please input it again.');
end
if (nargin==1)
   disp(' You forget input the method of Wavelet! The default method is
discrete Meyer Wavelet. If you want to use another wavelet.Please input
it again.');
   N =4;
end
```

```
if ((size(PrePulse,1)~=1))
  number=size(PrePulse,1);
else
  number=size(PrePulse,2);
end


for i=1:N
  SmoothPulse(i)=PrePulse(i);
end
for i=N+1:(number-N)
  SmoothPulse(i)=1/(2*N+1)*sum(PrePulse((i-
N):(i+N)));%%sum(newpulse((i-N):(i+N)))
end
for i=(number-N):number
  SmoothPulse(i)=PrePulse(i);
end

y=SmoothPulse; % return the result of function --smoothing
```

5.WAVELETBASE CODE

```
function
[newpulse,baseline]=waveletbase(pulse,wname,n,Extension,Choice)
%PrePulse)

%This function aimed at computing the wavelet coefficients of the pulse
% input_____wname: the name of the mother wavelet that you
want to use
```

```
%           |____pulse: the pulse signal to be processed
%           |____n:     the level that you want to compute the baseline
%           |____Extension: occasionally is 100's multipication . we suggest
to use 200
%           |____Choice 1. Assymetric extension
%                      2 Header and end extension
%                      3 Zero extension
%                      4 Attenuation extension
%
%
%
%
% output      waveletcoef        the wavelet coefficient of the pulse
%pulse=basechange(PrePulse);


if ((size(pulse,1)~=1))
else
  temp=pulse';
  pulse=temp;
end

OriginalPulse=pulse;
Num=length(pulse);


switch(Choice)
   case(1)
              if Extension==0
```

```
        signal=pulse';
            else
                    if (floor(Num/Extension)>=1)
          signal=[fliplr(pulse(1:Extension)')  pulse'  fliplr(pulse(Num-
Extension+1:Num)')];
                     else
          signal=[fliplr(pulse') pulse' fliplr(pulse')];
                    end
            end

  case(2)
    if Extension==0
        signal=pulse';
            else
                    if (floor(Num/Extension)>=1)
          a(1:Extension)=pulse(1);
          b(1:Extension)=pulse(end);
          signal=[a pulse' b];
                    else
          a(1:Num)=pulse(1);
          b(1:Num)=pulse(end);
          signal=[a pulse' b];
                    end
            end


  case(3)
    if Extension==0
        signal=pulse';
```

```
    else
            if (floor(Num/Extension)>=1)
        a(1:Extension)=0;
        b(1:Extension)=0;
        signal=[a pulse' b];
            else
        a(1:Num)=pulse(1);
        b(1:Num)=pulse(end);
        signal=[a pulse' b];
            end
    end



case(4)
  if Extension==0
     signal=pulse';
        else
            if (floor(Num/Extension)>=1)
       for i=1:Extension
          a(i)=(i-1)/(Extension-1)*pulse(1);
          b(i)=(Extension-i)/(Extension-1)*pulse(Num);
       end
       signal=[a pulse' b];
            else
       for i=1:Num
          a(i)=(i-1)/(Num-1)*pulse(1);
          b(i)=(Num-i)/(Num-1)*pulse(Num);
       end
```

```
            signal=[a pulse' b];
        end
            end


    otherwise
        disp('The choice of the extension only has four method.');
        disp('Please enter   1 ---asymmetric extension');
        disp('               2 --- header and endextension');
        disp('               3 --- zeroextension');
        disp('               4--- attenuation extension');
        error('Please enter the choice again!')
end

pulse=signal;
[c,l]=wavedec(pulse,n,wname);


% figure
if ((size(pulse,1)~=1))
   t=1:size(pulse,1);
else
   t=1:size(pulse,2);
end

NewSignal=pulse-wrcoef('a',c,l,wname,n);%-wrcoef('d',c,l,wname,1);
Baseline=wrcoef('a',c,l,wname,n);
% subplot(2,1,1);
% plot(t,pulse);
```

```
% grid on;
% title('pulse');
% subplot(2,1,2);
% plot(t,NewSignal);
% grid on;
% title('NewSignal');

% figure;
% plot(Baseline);
% title('Baseline did not being cut');
% grid on;

if Extension==0
   newpulse=NewSignal(Extension+1:Num+Extension);%-
wrcoef('d',c,l,wname,1);
   baseline=Baseline(Extension+1:Num+Extension);
else
       if (floor(Num/Extension)>=1)
       newpulse=NewSignal(Extension+1:Num+Extension);%-
wrcoef('d',c,l,wname,1);
       baseline=Baseline(Extension+1:Num+Extension);
       else
       newpulse=NewSignal(Num+1:Num+Num);%-
wrcoef('d',c,l,wname,1);
       baseline=Baseline(Num+1:Num+Num);
       end
end
baseline=smoothing1(baseline,10);
newpulse=OriginalPulse'-baseline;
```

```
% figure;
% subplot(2,1,1);
% plot([1:Num],OriginalPulse);
% grid on;
% title('pulse');
% subplot(2,1,2);
% plot([1:Num],newpulse);
% grid on;
% title('newpulse');
% figure;
% plot(baseline);
% title('baseline');
% grid on;
% % save decmp decmp;
% figure;
% plot([1:Num],OriginalPulse,[1:Num],baseline);
% title('original pulse and its baseline');
```

6. FINAL MAIN CODE

```
clc
clear all
close all
addpath('support')
cd DATABASE
[filename, pathname] = uigetfile('*.dat', 'Open file .dat');% only image
Bitmap
if isequal(filename, 0) || isequal(pathname, 0)
   disp('File input canceled.');
  ECG_Data = [];
```

```
else
fid=fopen(strcat(pathname,filename),'r');
end;
time=10;

f=fread(fid,2*360*time,'ubit12');
cd ..

Orig_Sig=f(1:2:length(f));
Orig_Sig=Orig_Sig./max(Orig_Sig);
subplot(4,1,1),plot(Orig_Sig,'r'),title('Original Signal')
% hold on

%%% adding EMG noise

%%% EMG noise is gaussian noise with zero mean and standard
deviation 10%

sigma=0.10;
e=Orig_Sig+rand(size(Orig_Sig)).*sigma;
subplot(4,1,2),plot(e,'g');title('Noisy Signal')
% title('Noisy ECG Signal');ylabel(' ---- n(t)');

%%%%%%%%%%%%%%%%%%%%%%%%%%%%%%%%%%%%%%%%% applying LMS
%%%%%%%%%%%%%%%%%%%%%%%%%%%%%%%%%%%%%%%%%%%%%%%%%%%%%%%%%

d=e;
x2=Orig_Sig;
N=length(x2);
```

```
N=length(e);
mu=0.5;
%_____________________
%------ start of the algorithm
w=zeros(1,N-1)';
w(1)=rand(1);
for i=1:N-1
    w1(i)=d(i)-w(i)'*e(i);
    w(i+1)=w(i)+mu*w1(i)*e(i);
end
out1=w(:).*e(:);



subplot(4,1,3),plot(out1);title('LMS Output')



%%%%%%%%%%%%%%%%                                    NLMS
%%%%%%%%%%%%%%%%%%%%%%%%%%%%%%%%


d=e;
x2=Orig_Sig;
N=length(x2);
mu=.01;
%_____________________
%------ start of the algorithm ========
```

```
w=zeros(1,N-1)';
w(1)=rand(1);
p=0.1;
for i=1:N-1
    er(i)=d(i)-w(i)'*x2(i);
    w(i+1)=w(i)+(mu*er(i)*x2(i))./(p+(x2(i)'*x2(i)));      %%      weight
updation
end

out1=w(:).*x2(:);

subplot(4,1,4);plot(out1);
title('NLMS ECG Signal');ylabel(' ----n(t)');
figure,
PSNR1=0;
for itr=1:10

   for i=1:N-1
     w1(i)=d(i)-w(i)'*e(i);
    w(i+1)=w(i)+mu*w1(i)*e(i);
   end

out1=w(:).*e(:);

[MSE1(itr) PSNR1(itr)]=evaluate_denoising_metric(Orig_Sig,out1,itr)

end
PSNR_LMS=mean(PSNR1)
MSE_LMS=mean(MSE1)
```

```
itr=1:10;
plot(itr,PSNR1,'r',...
       'LineWidth',5,...
    'MarkerSize',10,...
    'MarkerEdgeColor','b',...
    'MarkerFaceColor',[0.5,0.5,0.5])
xlabel('Number of Iterations')
ylabel('PSNR(in db)')
grid on
hold on
title('Number of Iterations vs PSNR Plot')

PSNR2=0;
for itr=1:10

   for i=1:N-1
    er(i)=d(i)-w(i)'*x2(i);
    w(i+1)=w(i)+(mu*er(i)*x2(i))./(p+(x2(i)'*x2(i))).*itr;    %%    weight
updation
   end

out1=w(:).*x2(:);

[MSE2(itr) PSNR2(itr)]=evaluate_denoising_metric(Orig_Sig,out1,itr);
end

PSNR_NLMS=mean(PSNR2)
MSE_NLMS=mean(MSE2)
```

```
itr=1:10;
plot(itr,PSNR2,'g',...
       'LineWidth',5,...
    'MarkerSize',10,...
    'MarkerEdgeColor','b',...
    'MarkerFaceColor',[0.5,0.5,0.5])
% xlabel('Number of Iterations')
% ylabel('PSNR(in db)')
% grid on
hold off
legend('LMS','NLMS')
% title('Number of Iterations vs PSNR Plot')


figure,

plot(itr,MSE1,'r',...
       'LineWidth',5,...
    'MarkerSize',10,...
    'MarkerEdgeColor','b',...
    'MarkerFaceColor',[0.5,0.5,0.5])

grid on
hold on
plot(itr,MSE2,'g',...
       'LineWidth',5,...
    'MarkerSize',10,...
    'MarkerEdgeColor','b',...
    'MarkerFaceColor',[0.5,0.5,0.5])
```

```
xlabel('Number of Iterations')
ylabel('MSE')
grid on
hold off
title('Number of Iterations vs MSE Plot')
legend('LMS','NLMS')

plot(PSNR2,MSE2),hold on

plot(PSNR1,MSE1)
legend('NLMS','LMS')
grid on
title('PSNR-MSE Performance Graph ')
xlabel('PSNR')
ylabel('MSE')
```